Insight into a Mechanism Generating Cyclic di-GMP Heterogeneity in *Pseudomonas aeruginosa*.

Bridget R. Kulasekara

A dissertation

submitted in partial fulfillment of the

requirements for the degree of

Doctor of Philosophy

University of Washington

2013

Reading Committee:

Samuel I. Miller, Chair

Caroline S. Harwood

Lucas R. Hoffman

Program Authorized to Offer Degree:

Molecular and Cellular Biology

University of Washington

Abstract

Insight into a Mechanism Generating Cyclic di-GMP Heterogeneity in *Pseudomonas aeruginosa*.

Bridget R. Kulasekara

Chair of the Supervisory Committee:

Professor Samuel I. Miller

Department of Medicine, Microbiology, and Genome Sciences

Phenotypic heterogeneity is a commonly observed phenomenon in cell populations that can provide a selective advantage within diverse, unpredictable conditions. Second messenger-based signaling, having a global impact on cellular physiology, can be a mechanism by which environmental signals are rapidly translated into phenotypic heterogeneity. However, such mechanisms for generating phenotypic heterogeneity have yet to be described for many cell types, including bacteria. In biology heterogeneity within populations is often overlooked, as most biochemical characterizations utilize bulk populations of cells for analyzes. The second messenger c-di-GMP (CDG) regulates diverse bacterial processes, including cell-cycle progression, motility, and exopolysaccharide production, and in human cells, innate immunity.

Previously, using a FRET-based biosensor and microscopy, we observed that individual bacterial cells demonstrated heterogeneity in CDG levels within populations; however the precise mechanism by which this diversity is generated was unknown. Here we show that CDG heterogeneity in *Pseudomonas aeruginosa* is promoted by a CDG specific phosphodiesterase partitioned after cell division by the chemotaxis machinery. We found that reduction of CDG levels by this phosphodiesterase is dependent on components of the chemotaxis machinery, including the histidine kinase CheA. We observed that both the chemotaxis machinery and the phosphodiesterase are partitioned predominantly into the flagellated progeny. The phosphorylation of CheA is required for phosphodiesterase activity, indicating that chemotaxis signals could affect CDG degradation, thereby altering bacterial motility. Our work demonstrates that cellular heterogeneity can be generated through a second messenger whose concentration is regulated by a combination of environmental signals and the asymmetrical inheritance of organelles. Second messenger heterogeneity is likely an important mechanism for many biological processes occurring in a variety of cell types, including malignant cells, immune cells, and single cell organisms.

Table of Contents

Page

List of Figures

List of Tables

Acknowledgements

I would like to express my gratitude to my advisor, Dr. Samuel Miller, for his mentorship and guidance. I am especially grateful for his enthusiasm, advice, understanding, and knowledge. I am grateful to my committee members, Drs. Caroline Harwood, Lucas Hoffman, Rachel Klevit, and Barry Stoddard for their advice and helpful discussion. I am sincerely appreciative of the members of the Miller Lab that have made significant contributions to this project, including Dr. Matthias Christen, Dr. Hemantha Kulasekara, Cassandra Kamischke and Richard Pfuetzner. I would like to thank the Paul Wiggins lab for providing their custom written software for the analysis of microscopy data and Dr. Paul Wiggins for providing advice on data analysis. I am thankful for the assistance provided by Dr. Dan Fong and Gary Davis of Nikon Instruments who set up our microscopy system and provided support since that period. I would like to thank the individuals that have mentored me in an unofficial capacity including Dr. David D'Argenio, Dr. Mitchell Brittnacher, Dr. Lucas Hoffman, Dr. Heather Felise, and Dr. Anu Chaudary. I would like to express my appreciation to Dr. Stephen Lory, who mentored me while I worked in his lab as a technician prior to entering graduate school. Finally, I am indebted to my family, especially my husband Hemantha, for their love, understanding, and support.

Chapter 1. Introduction

Historical Perspective

c-di-GMP (CDG) is a secondary signaling molecule in bacteria that controls a variety of functions including flagellar motor control, exopolysaccharide and adhesion production, and *C. crescentus* morphogenesis (Römling et al., 2013; Sondermann et al., 2012). Moshe Benziman and colleagues discovered the molecule CDG almost 25 years ago when they identified it as an allosteric activator of *Gluconacetobacter xylinus* cellulose synthase (Ross et al., 1987). Subsequent characterization of enzymes with CDG biosynthetic and degradative properties determined that the GGDEF domain confers CDG synthesis activity, termed diguanylate synthase or DGC, and the EAL and HD-GYP domains confer CDG degradation activity, termed phosphodiesterase or PDE (Paul et al., 2004; Tischler and Camilli, 2004; Simm et al., 2004). During the early phase of microbial genome sequencing, the widespread nature of these previously uncharacterized domains in microbes, first referred to as DUF1 and DUF9 for DGC and PDE respectively, was noted and discussed in several reviews (Galperin et al., 2001) (Galperin, 2001). When their functions were assigned, researchers began to speculate about a more universal role for CDG (Jenal, 2004). Since then, mutant analysis of DGC and PDE encoding genes have led to a commonly cited paradigm in which CDG acts as a binary switch to control bacterial motility and sessility.

General Themes of DGCs and PDEs

In general, the domains that confer enzymatic activity are widely conserved across many classes of bacteria. However, these enzymes utilize a modular architecture where diverse sensory domains are located at the N-terminus and GGD/EEF and EAL domains are located at the C-

terminus. Common sensory domains include PAS, REC, and GAF domains that modulate activity in response to ligand binding, phosphorylation, or protein-protein interactions. PAS (Per-ARNT-Sim) domains mediate ligand binding or protein-protein interactions (Henry and Crosson, 2011). One of the most common signal transduction systems in bacteria is the two-component system consisting of the histidine kinase and response regulator. Histidine kinases sense and respond to environmental signals by phosphorylating a cognate response regulator. Rec domains are a defining component of response regulators and are phosphorylated at a conserved aspartate residue resulting in altered gene transcription or other processes (Jung et al., 2012). GAF domains (first found in cGMP-specific phosphodiesterases, adenylyl cyclases and E. coli FhlA) mediate protein-protein interactions and bind small molecules. They are found in cGMP and cAMP specific PDEs where their binding to cyclic nucleotides stimulates PDE activity (Heikaus et al., 2009). In spite of low sequence conservation, there are common patterns of domain organization, including PAS-GGDEF, GAF-GGDEF, Rec-GGDEF, and Rec-Rec-GGDEF, suggesting conserved modes of regulation (Römling et al., 2013). Regulators of enzymatic activity may be encoded with the enzyme as part of an operon (Malone et al., 2010; Hickman et al., 2005). Additionally, PDEs often possess an inactive GGDEF domain, as indicated by lack of residues important for catalysis, in combination with an EAL domain. The GGDEF when bound to GTP activates PDE activity (Christen et al., 2005; Seshasayee et al., 2010). Very few characterized proteins to date possess both PDE and DGC enzymatic activities including *Rhodobacter sphaeroides* BphG1 (Tarutina et al., 2006), *Vibrio parahaemolyticus* ScrC (Ferreira et al., 2008; Boles and McCarter, 2002; Trimble and McCarter, 2011), and *Mycobacterium smegmatis* MSDGC-1 (Bharati et al., 2012).

Mechanism of DGC and PDE Activity

Much of what is known about DGC function and regulation was provided from the structure of the *C. crescentus* DGC PleD (Chan et al., 2004; Wassmann et al., 2007) (Figure 1 and 2).The formation of CDG from GTP requires two antiparallel GTP-loaded GGDEF domains. Catalysis most likely involves deprotonation of the 3'-OH group of GTP to allow an intermolecular nucleophilic attack on the α-phosphate of the second GTP substrate. A conserved lysine (K332) likely stabilizes the charge of the developing pentacoordinated phosphoryl transition state and the pyrophosphate leaving group (Figure 2). This domain is part of the class III nucleotidyl cyclase family; where other members include adenyl cyclases that synthesize cAMP from ATP. Like adenyl cyclases, DGCs may utilize a metal assisted mechanism to form phosphodiester bonds. The third residue in the GGD/EEF motif, E370 and a conserved aspartate D327 both associate with Mg2+ whereas the fourth residue in the GGD/EEF motif, E371 may serve a similar role. Details of the DGC catalytic mechanism remain unresolved as researchers have been unable to solve the structure of an active DGC homodimer.

Common modes of allosteric regulation occur through product mediated feedback inhibition and Rec domain phosphorylation. PleD consists of two tandem Rec domains (D1 and D2) N-terminal to the GGD/EEF domain (where the eponymous motif is located from positions 368-372). Phosphorylation of the D1 Rec domain is required for activity of PleD. Structural characterization revealed that phosphorylation of D1 produces a structural rearrangement that induces repacking of the D1-D2 interface and facilitates dimerization. Allosteric inhibition occurs through CDG binding to the I-site of PleD that consists of the RxxD motif five residues upstream of the GGD/EEF motif. The two structures of PleD in complex with CDG show that I-site occupancy may act to stabilize an intramolecular interaction between the D2 and GGD/EEF

domains or act to form intermolecular crosslinks between two DGC domains. Both events likely function to reduce the probability that two substrate loaded GGD/EEF domains will interact in a manner required for catalysis.

The structure of the PDE, BlrP1, has revealed that catalysis may involve the antiparallel association of two EAL domains and proceeds utilizing a two metal catalytic mechanism similar to that of other cyclic nucleotide PDEs (Barends et al., 2009) (Figure 1 and 2). A water molecule bridges two metal ions and initiates a nucleophilic attack on a phosphorus atom. O3 is then expulsed following protonation by a second water molecule (Figure 2). The first metal ion is coordinated by eight atoms including those from four EAL domain residues whereas the second metal ion is coordinated in a trigonal-bipyramidal manner including atoms from three EAL domain residues. When present in tandem with a degenerate GGD/EEF domain, PDE activity is often stimulated upon binding to GTP (Christen et al., 2005). Other modes of allosteric regulation have also been characterized. It is thought that allosteric regulation acts to induce a conformational change that optimizes the positions of catalytic residues (Barends et al., 2009).

Themes in Effector Binding

Using bioinformatics to analyze DGC and PDE encoding genes and data mining of published manuscripts, Galperin suggested in 2006 that the elusive CDG receptor is conferred by the PilZ domain (Amikam and Galperin, 2006). He noted that the cellulose synthase BcsA protein that requires CDG for allosteric activation contains a domain homologous to the PilZ protein from *P. aeruginosa*. *P. aeruginosa pilZ* mutants are defective for twitching motility as are *fimX* mutants (Mattick, 2002; Huang et al., 2003). The *P. aeruginosa* FimX protein contains both a DGC and PDE domain. Additionally, the motility defect of an *hns* mutant of *Salmonella*

can be overcome by a suppressor mutation in the PilZ domain encoding gene *ycgR* or overexpression of an EAL domain containing protein *yhjH* (Ko and Park, 2000). Subsequent genetic studies of the PilZ domain encoding genes confirmed that PilZ domain is indeed one of the CDG binding receptors (Ryjenkov et al., 2006). Since then, a plethora of other CDG binding receptors have been identified. These CDG binding effector proteins often couple domains that confer CDG binding with domains that enable diverse modes of output such as DNA binding (Johnson et al., 2011; Krasteva et al., 2010) or type 2 glycosyltransferase activity (Solano et al., 2002). Multiple domains are now known to confer CDG binding ability, including GGDEF (Chan et al., 2004), degenerate EAL (Navarro et al., 2009), PilZ (Ryjenkov et al., 2006), non-canonical Rec (Krasteva et al., 2010), CRP (Chin et al., 2010) domains and RNA based riboswitches (Smith et al., 2009). Common motifs that confer binding are characterized by the presence of arginine residues, such as RxxxR in the PilZ domain (Sondermann et al., 2012), RxxD in the GGDEF domain I-site (Chan et al., 2004), and W[F/L/M][T/S]R in the VpsT Rec domain (Krasteva et al., 2010). Structural studies have revealed that the positively charged side chain often associates with the phosphate group and guanine base of CDG to confer structural complementarity (Benach et al., 2007).

YcgR, a Characterized Example of CDG Signaling

High levels of CDG inhibit swimming motility in numerous species. In *E. coli*, this inhibition is achieved through binding of CDG to its effector, YcgR. Homologs of YcgR exist in a diverse array of bacteria, including *Vibrio cholera*, *P. aeruginosa,* and *C. crescentus*. YcgR binds CDG with an affinity of ~200 nM to its PilZ domain. In 2010, three manuscripts were published each describing different modes of action.

Boehm et al. (2010) proposed a model where YcgR in complex with CDG acts to inhibit swimming motility by reducing the speed of flagellar rotation in *E. coli*. The YcgR/CDG complex was proposed to act on the proton channel, MotA that converts proton motive force to mechanical energy by rotating the flagellar rotor. YcgR/CDG was proposed to act in a brake like fashion as cells with increased levels of CDG did not exhibit passive rotation when tethered to a surface. YcgR was determined to directly bind the stator, as evidenced by suppressor point mutants isolated in MotA and FRET exhibited between two fluorophores fused to a fragment of the stator (MotA) and YcgR. These authors also observed increased colocalization of YcgR and rotor protein FliM in the presence of high CDG, indicating that CDG bound to YcgR promotes complex formation with the stator. They determined a physiological relevance for the effect of CDG on motility by showing that decreased swimming motility speeds observed during entry into stationary phase are mediated by YcgR.

In contrast to this mechanism of action, work by Xin Fang and Mark Gomelsky (Fang and Gomelsky, 2010) supported a model where YcgR causes counter clockwise bias of flagellar rotation when bound to CDG. The effects of YcgR bound to CDG were determined by monitoring the rotational bias of tethered cells. These authors hypothesized that YcgR acts by binding to a component of the flagellar apparatus, and then used purified YcgR to probe for binding partners in bacterial lysates from cells that had ectopically expressed flagellar rotor and MS ring components. Using this approach, these authors identified FliG as a binding partner for YcgR. Utilizing the bacterial two-hybrid system, they determined that the YcgR/FliG interaction is enhanced in the presence of CDG. FliG residues required for YcgR binding were subsequently identified and mapped onto the face of the FliG structure.

Paul et al. (2010) presented a mechanism with elements similar to both of the other manuscripts. These authors measured the rotational bias and rotational speed of tethered cells to determine that YcgR promotes a counter clockwise bias and slows the rotation of the flagellum in response to CDG binding. They employed a similar approach to that used by Fang et al. (2010) to test whether YcgR interacts with the flagellar MS-ring, rotor, or MotA, and determined YcgR interacts with FliG and FliM. They subsequently characterized residues in FliG, FliM, and YcgR that were important for CDG mediated YcgR activity and used microscopy to determine that YcgR localizes to the flagellar apparatus in a CDG dependent fashion. Ultimately, a backstop brake model was derived, where YcgR acts to both reduce flagellar rotation and inhibit switching to clockwise rotation by inducing a conformational change in FliG. This model presents what could be a consensus of the mechanism by which YcgR inhibits motility. All three studies agreed that CDG strengthens the interaction with its respective binding partner; however the mode by which YcgR acts is not conclusive. Further biochemical, genetics and structural studies will need to be performed to determine the identity of the YcgR binding proteins.

CDG Signaling Specificity

Bacterial genomes often encode numerous effector proteins. Therefore, there are multiple biological outcomes affected by this signaling molecule (Römling et al., 2013). With the large number of biological outcomes, how is signaling specificity achieved? A similar question has been asked about cAMP signaling in eukaryotic cells. This molecule mediates an array of diverse processes such as cell cycle regulation, chromatin condensation, and nuclear envelope disassembly (Taskén and Aandahl, 2004). Its effects are modulated by cAMP-dependent protein kinase A (PKA) which is a heterotetramer of two catalytic and two regulatory subunits. The

combination of subunits determines the affinity for cAMP. It was postulated over 40 yrs ago that signaling specificity is achieved through localized pools of cAMP (Kuo and Greengard, 1969). This hypothesis was puzzling when considering the rapid diffusion of a small molecule such as cAMP but provided an answer as to how this molecule affects numerous biological outputs within a single cell (Taskén and Aandahl, 2004). Direct evidence in support of subcellular pools of cAMP came from the development of a biosensor which demonstrated significant gradients occurring over a distance as small as 1 micron within cells (Zaccolo and Pozzan, 2002). However, this finding was not supported by data from cAMP biosensors of different design that showed much more minor variations of cAMP mostly existing at the cell membrane (Terrin et al., 2006; Rochais et al., 2006).In spite of these unknowns, cAMP compartmentalization has become an accepted explanation of the signaling specificity conundrum (Conti and Beavo, 2007). One hypothesis about how putative cAMP gradients are achieved is through the action of specific PDEs (Terrin et al., 2006). Computational simulations of spatial variation in cAMP found that gradients could be established when a pool of PDE4D was anchored in the cytosol (Oliveira et al., 2010). An alternative model is that adenylyl cyclase and receptor molecules are localized together in a complex that also impedes diffusion of the signaling molecule before it reaches its target (Davare et al., 2001). Overall, cAMP microdomain formation in eukaryotic cells is an active area of research.

A similar hypothesis has been proposed for CDG signaling specificity in bacteria by Hengge (2009). Merritt et al. (2010) and Massie et al. (2012) both argue their data supports the existence of localized pools of CDG. Merrit et al. (2010) characterized phenotypes in two DGC mutants. These authors determined that although the two mutants exhibit different phenotypic variation, both mutants exhibited similar reported decreases in total CDG levels when extracted

from bulk cultures. As they were unable to correlate CDG levels with phenotypic behavior, the authors concluded their results support the existence of subcellular pools of CDG. There are several alternative explanations for this observation, two of which will be outlined in further detail.

The authors measured CDG from cells grown to stationary phase to determine whether this enzyme had an effect on the global pool of CDG. As they observed no difference between the mutant and the wild type, they concluded that this enzyme must generate subcellular pools of CDG. However, this conclusion may have been premature as they didn't actually test CDG levels under conditions that lead to a phenotypic difference between the mutant and the wild type. Secondly, measured CDG levels from bulk culture could reportedly be the same but come from distinct population distributions of CDG (for a discussion, refer to (Altschuler and Wu, 2010)).

Massie et al. (2012) employed a novel use of flow cytometry to measure cellular aggregation as a readout of the effects of CDG in *Vibrio cholerae.* They determined that ectopic expression of individual DGCs from the same artificial promoter resulted in different degrees of cellular aggregation. They subsequently quantified CDG from each DGC expressing strain in the presence of various amounts of inducer and failed to identify a significant linear correlation between total CDG and cellular aggregation. However, when they grouped the varying expression level data according to individual DGC, cellular aggregation was much more significantly correlated to overall CDG levels as explained by the observation that expression of each DGC gave rise to a different slope when fitting a line to cellular aggregation versus CDG concentrations. The authors' explanation for this result was that CDG must be acting through subcellular pools to achieve signaling specificity. An alternative explanation for these

observations is that each DGC was active in only a fraction of cells. Therefore, expression of each DGC resulted in a unique subset of cells exhibiting a DGC specific increase in CDG. A shallower slope could therefore be a result of DGC activity in a smaller population of cells. This hypothesis is quite plausible, as the occurrence of allosteric regulation has been shown for several DGCs (Christen et al., 2010; Malone et al., 2010; Hickman et al., 2005). Furthermore, published results indicate that these allosteric regulatory events can be limited to specific subpopulations (Viollier et al., 2002; Wheeler and Shapiro, 1999; Paul et al., 2004; O'Connor et al., 2012).

CDG signaling specificity achieved by coupling cellular CDG concentrations with distinct affinities of effector molecules is a hypothesis backed by more compelling evidence. Pultz et al. (2012) and Shikuma et al. (2012) both show evidence that the cellular concentration of CDG affects biological output. By modulating the affinities of two proteins that 1) mediate inhibition of swimming motility (YcgR) and 2) mediate cellulose production (BcsA) in combination with altering cellular CDG levels, Pultz et al. (2012) demonstrated that biological outcome is directly related to cellular concentration and effector affinity. This author also characterized several *P. aeruginosa* effectors demonstrating their affinities exist over a wide range of concentrations. This observed diversity in effector affinity again supported the hypothesis that specificity is achieved by coupling cellular CDG concentrations with distinct affinities of effector molecules.

Shikuma et al. (2012) performed a similar study looking at CDG dependent DNA binding of the *Vibrio Cholera* protein VpsT. As the number of functional DGCs in the cell increased, subcellular localization of VpsT also increased. They could replicate the correlation between

increased DGC expression and VpsT localization in a heterologous host. Their finding supported the idea that CDG affects biological output through modulating cellular concentrations.

Signaling specificity can be also achieved by differential expression or partitioning of individual components of CDG signaling cascades. In this mode of regulation, for a given environmental condition, specific DGCs, PDEs and receptor components are expressed (Weber et al., 2006). Along the same line of thought are the DGCs, PDEs, and receptors that act in a specific cell population. This mode of signaling specificity can be also coupled to spatio-temporal activation of particular DGC and PDE enzymes that give rise to bursts of CDG signaling molecules during certain segments of bacterial cell cycle. The generation of CDG asymmetry by *C. crescentus* occurs in part through the unequal partitioning of a DGC, PleD, to the pole of the incipient stalked cell that maintains higher CDG levels (Christen et al., 2010; Paul et al., 2004). In contrast to many other well studied Gram-negative bacteria, *C. crescentus* exhibits an asymmetric cell cycle in that the two daughter cells have unique morphologies and functions. Only the daughter swarmer cell with a polar flagellum is motile, and only the stalked cell, with the exopolysaccharide containing holdfast can undergo cell division (Tsokos and Laub, 2012). PleD is essential for the holdfast formation of the stalk. PleD mutants cannot undergo swarmer to stalked cell transition or eject pili and flagella and therefore remain as motile swarmer cells. In order for PleD to localize to the incipient stalked cell pole, it must be phosphorylated by the DivJ kinases (Paul et al., 2004); however the features that distinguish this cell from the other cell pole and facilitate preferential PleD localization are unknown. It has been assumed that the asymmetry between the two cells provides inherent polarity for the preferential localization of PleD to the incipient stalked cell (Paul et al., 2004). Additionally, PdeA phosphodiesterase activity is limited only to the swarmer cell by regulated proteolysis in the

stalked cell, which ensures optimum CDG levels for flagella based motility in the swarmer cell. Two CDG receptor proteins have been identified that are important for morphogenesis. TipF is a putative CDG binding protein implicated in flagella assembly (Huitema et al., 2006). PopA, a homolog of PleD in which the catalytic site for DGC activity is degenerate, binds CDG and localizes to the stalked pole, and interacts with proteases to degrade the master cell cycle control regulator CtrA (Duerig et al., 2009).

Other than the example of *C. crescentus* in which the dividing cells are remarkably morphologically different, little is known about individual variation of microbes as a product of cell division. Often the possibility of heterogeneity is evoked to explain surprising phenotypes, such as microbial antibiotic tolerance, or variability in the susceptibility of bacterial populations to antibiotics (Dhar and McKinney, 2007; Aldridge et al., 2012). Current knowledge suggests variation resulting from cell division could occur through several mechanisms including inherent cellular polarity (Dworkin, 2009). Each bacterial cell has a new and old pole as a result of cell division. The new pole is physiologically distinguished from the old pole by the remnants of the divisome and newly synthesized peptidoglycan (Pedro et al., 1997). These biochemical markers may serve as cues for proteins to preferentially localize to a single pole, creating heterogeneity. Cellular heterogeneity can also result from processes that are stochastic including mutations, unequal partitioning of less abundant proteins (Elowitz et al., 2002), or alteration in gene expression as a result of phase variation due to DNA modifying enzymes (Woude, 2011). This work (Chapter 4) introduces how unequal partitioning of an enzyme may control organelle function in *P. aeruginosa*.

Pseudomonas aeruginosa

Pseudomonas aeruginosa is a gram-negative gammaproteobacterium found in numerous environments. This bacterium is an opportunistic pathogen that causes infections in immunocompromised individuals, in individuals with cystic fibrosis, and in association with abiotic surfaces as part of medical devices such as catheters, ventilators, and implants (Gibson et al., 2003; Park, 2005). *P. aeruginosa* is inherently resistant to multiple antibiotics due to its relatively impermeable outer membrane coupled with the presence of efflux pumps and possession of enzymes that degrade or modify antibiotics or increase copy number of the target (Lister et al., 2009). *P. aeruginosa* also forms biofilms, characterized as exopolysaccharide encased communities of bacteria, during infection of cystic fibrosis patients and in association with medical devices. These types of infections are especially recalcitrant to treatment.

A Brief Description of Characterized DGCs and PDEs in *P. aeruginosa*

Kulasekara et al (2006) utilized transposon insertion mutants and overexpression constructs to perform a genome-wide characterization of putative DGCs and PDEs in *P. aeruginosa* (Table 1). Enzymatic activity was determined by analyzing extracts following expression in *P. aeruginosa* and detecting and quantifying CDG using HPLC. Biological effects from abrogating genes as well as overexpression were characterized by quantifying biofilm formation, motility and cytotoxicity. This manuscript determined that as a general theme, CDG contributes to biofilm formation and inhibits virulence in *P. aeruginosa*. The genes that were determined to encode DGCs included PA0847, PA1107, PA1120, PA1727, PA2870, PA3343, PA3702, and PA5487. The genes that were determined to encode PDE activity included PA2133, PA2200, PA3825, PA3947, and *pvrR*. Subsequent genetic work carried out by other groups has elucidated detailed phenotypes and functions of these enzymes, which are listed below.

DGCs

SiaD (PA0169) is required for *P. aeruginosa* to generate an autoaggregative response to SDS (Klebensberger et al., 2009) and for increased CDG levels in response to psl exopolysaccharide (Irie et al., 2012). SiaD is the last gene transcribed as part of a 4-gene operon (PA0172-PA0169), and its enzymatic activity may be stimulated by the inner membrane protein SiaA (PA0172) in response to an unknown periplasmic signal. SiaA contains a periplasmic sensing domain, a HAMP domain and a PP2C-like phosphatase domain (Klebensberger et al., 2009).

RoeA (PA1107) is a DGC required for biofilm and exopolysaccharide production in PA14. RoeA stimulates pel exopolysaccharide production most likely through a post-translational mechanism as it does not affect transcription of exopolysaccharide genes (Merritt et al., 2010). Mutants in RoeA also exhibit a 2-fold increased swarming motility. A fusion of GFP to RoeA shows it is located not quite diffusely throughout the cell (Merritt et al., 2010) suggesting it could associated with the inner membrane. In support of this observation, biochemical fractionation studies indicate this protein is localized to the inner membrane.

TpbB/YfiN (PA1120) YfiN is a membrane bound DGC with a periplasmic sensing PAS domain and cytoplasmic HAMP and GGDEF domain. Activity of YfiN is modulated by two additional periplasmically localized proteins. The periplasmically soluble protein YfiR is required for repression of YfiN and the outer membrane lipoprotein, YfiB, is required for activation of YfiN. Biochemical and genetic data suggest YfiN is suppressed by directly binding YfiR where this interaction is disrupted when YfiB sequesters YfiR to the outer membrane (Malone et al., 2012; Malone et al., 2010). YfiN activation contributes to small colony variant (SCV) formation in clinical isolates through mutations in either *yfiR* or *yfiN*.

WspR (PA3702) is required for biofilm formation (D'Argenio et al., 2002; Hickman et al., 2005) and its activation contributes to SCV formation in clinical isolates through inactivating mutations in *wspF* (Smith et al., 2006).This protein is part of a signaling complex that belongs to the alternative cellular function chemotaxis family with functions paralogous to the chemotaxis machinery. Members of this family form protein complexes that function to detect signals in the periplasm and transmit this information to a response regulator-like protein in the cytoplasm. In this instance, the receiver domain of the DGC, WspR, is phosphorylated by the kinase, WspE where WspR phosphorylation activates DGC activity (D'Argenio et al., 2002; Hickman et al., 2005). Inactivating mutations of *wspF*, a protein that demethylates the transmembrane chemoreceptor like protein, WspA, therefore activate WspR (Hickman et al., 2005) by stimulating WspR phosphorylation. *wspF* mutations also promote cluster formation of WspR, as measured by a fluorescent protein fusion, to the periphery of the cell (Guvener et al., 2006). Cluster formation is dependent upon residues involved in phosphorylation. Therefore, WspR cluster formation may reflect whether this DGC is active, however, this enzyme exhibits feedback inhibition due to CDG binding to the I-site and there are additional modes of regulating the enzymatic activity of WspR whose details are outlined in (Nabanita et al., 2008). Interestingly, WspR cluster formation forms in response to growth on solid surfaces, where cells grown in liquid exhibit much less frequent cluster formation (Güvener and Harwood, 2007) and is suggestive that cellular CDG levels are higher during growth on solid surfaces than in planktonic cells. The Wsp chemosensory system is localized to the inner membrane, and fluorescence microscopy of fusions to WspA shows that the chemosensory system is located at the periphery of the cell as expected but is also enriched at the poles of the cell (O'Connor et al., 2012).

SadC (PA4332) possesses several transmembrane domains and localizes to the inner membrane as determined by biochemical fractionation. Like SiaD, SadC is required for increase in CDG levels in response to psl exopolysaccharide (Irie et al., 2012). Mutants in this gene exhibit ~5-fold increased swarming motility and decreased exopolysaccharide production and biofilm formation where they are specifically affected during the transition from reversible to irreversible attachment (Merritt et al., 2007). SadC mutants also exhibit increased flagellar reversals (Merritt et al., 2007), consistent with the hypothesis that CDG promotes smooth swimming. A fusion of GFP to SadC exhibits a subcellular localization pattern consistent with its inner membrane localization and also exhibits preferential localization to the pole in a small fraction of cells (Merritt et al., 2010).

PDEs

RocR (PA3947) consists of an N-terminal Rec domain and C-terminal EAL domain. RocR is encoded at the same genomic location as *rocS1* and *rocA1*, three proteins that together share features of a two-component regulatory system. RocS1/RocA1 pair is responsible for activation of *cupC* fimbria and possibly other adhesive factors. RocS1 is a histidine kinase like protein that likely phosphorylates the RocR and RocA1 Rec domains. RocS1 is most likely membrane bound and autophosphorylates a His residue but is atypical in that it executes a His-Asp-His phosphorelay before phosphotransfer to Asp residues of RocR and RocA1. Genetic data suggests RocR is activated by phosphorylation (Kulasekara et al., 2005). The structure of RocR has been solved in its unphosphorylated form. This protein forms a tetramer with subunits that adopt two unique conformations. Structural data suggests that when not phosphorylated, the REC domain prevents access of CDG to two of the four catalytic EAL domains within the tetramer. It is

thought that phosphorylation may initiate a local conformational change such as a hinging between the REC and EAL domain to allow access of the substrate to the catalytic pocket (Chen et al., 2012).

RbdA (PA0861) is a PDE involved in biofilm dispersal. Mutants in this PDE exhibit increased biofilm formation and pel exopolysaccharide production and decreased swarming motility (An et al., 2010). This protein has N-terminal PAS-PAC domains and GGDEF and EAL domains. Measurements of activity from purified protein show it has PDE activity allosterically activated by GTP binding to the GGDEF domain. Surprisingly, this protein also synthesizes the linear dimeric GMP molecule pGpG from GTP; dependent upon the presence of both GGDEF and EAL domains. Biofilm formation is stimulated under anaerobic conditions; however, this effect is much greater in the absence of RbdA or in RbdA lacking critical residues of the PAS domain. This genetic evidence indicates that RbdA activity is stimulated in the absence of oxygen.

Arr (PA2818) Biofilm formation is stimulated upon exposure to sub-inhibitory concentrations of tobramycin. Mutants disrupted in *arr*, a PDE, do not form tobramycin induced biofilms, suggesting Arr activity occurs in response to aminoglycosides. Arr possesses a transmembrane segment and a domain localized to the periplasm that could potentially act to sense aminoglycosides. Arr, interestingly, is not encoded by all *P. aeruginosa* genomes, indicating PDE activity stimulated by aminoglycoside molecules is strain specific (Hoffman et al., 2005).

DipA/Pac (PA5017), the focus of the results section, was first characterized as important for flagellar motility where a mutant in this protein exhibited reduced swimming and swarming motility and a 2-fold increase in chemotaxis gene expression (*cheYZAB*) (Li et al., 2007). Using a model consisting of five day old biofilms in a plastic tubing, PA5017 was subsequently identified as being important for biofilm dispersion in response to addition of nutrients or

noxious signals (Roy et al., 2012). Results of *in vitro* endpoint assays of purified PA5017 suggest DGC activity is stimulated by another signaling molecule, cAMP where this response to cAMP requires the GAF domain of PA5017 (Roy et al., 2012). BdlA, another protein required for dispersion from biofilms has also been reported to indirectly interact with PA5017 as measured by co-immunoprecipitation experiments (Petrova and Sauer, 2012a). Although BdlA contains a typical MCP domain, it is not clear whether it interacts with the chemotaxis complex as it lacks a salient characteristic of MCP proteins; the transmembrane domains and has been reported to be in the soluble fraction of cell lysates. Additionally, BdlA is phosphorylated at a tyrosine residue and requires proteolytic cleavage for its activity, a phenomenon observed in cells dispersed from a biofilm but not during planktonic growth (Petrova and Sauer, 2012b).

BifA (PA4367): Mutants in *bifA* exhibit increased biofilm formation, increased pel exopolysaccharide production, and are defective in swarming motility. This mutant's increased biofilm forming phenotype may be due to its increased initial attachment at the air liquid interface. Biochemical fractionation shows BifA localizes to the inner membrane, as predicted by its encoded signal sequence and transmembrane segment (Kuchma et al., 2007).

Characterized Effectors in *P. aeruginosa*

FleQ (PA1097) is an enhancer binding protein that acts in complex with another protein, FleN to regulate genes involved in flagellar biosynthesis and biofilm formation (Hickman and Harwood, 2008; Arora et al., 1997; Dasgupta et al., 2003). This complex regulates transcriptional activity of σ^{54}-RNA polymerase as well as σ^{70}-RNA polymerase. FleQ/FleN acts to regulate a subset of genes transcribed by σ^{70}-RNA polymerase, including those required for pel and psl exopolysaccharide synthesis, in a CDG dependent fashion (Baraquet et al., 2012; Hickman and

Harwood, 2008). FleQ has three domains including an N-terminal FleQ domain, an AAA+ ATPase σ^{54} interaction domain, and a C-terminal helix turn helix DNA binding domain. In contrast to the *E. coli* mode of flagella transcriptional regulation, *P. aeruginosa* contains a four-tier flagella regulon, and FleQ/FleN/RpoN are at the top tier of this regulon. A model for CDG dependent repression by FleQ was developed by characterizing *in vitro* binding of FleQ to the *pel* exopolysaccharide promoter and *in vivo* studies of th e effect of various FleQ binding site mutants on transcription (Baraquet et al., 2012). FleQ binds two sites upstream of the *pel* translational start site and forms a one to one complex with FleN, which in turn binds ATP. In the absence of CDG, the complex induces DNA bending and prevents access of RNA polymerase to the promoter region. In the presence of CDG, the DNA bending by the FleQ/FleN complex is relieved. Furthermore, this model predicts repression of RNA polymerase is relieved at one binding site whereas FleQ/FleN in complex with CDG and ATP are thought to stimulate transcription by RNA polymerase σ^{70} at the other site. *In vitro* studies have shown that FleQ binds directly to CDG with an affinity of 15-20 μm, although the region of the protein that binds CDG hasn't yet been determined.

FimX (PA4959) is required for twitching motility that occurs via extension and retraction of the polar Type IV Pilus (Huang et al., 2003). FimX localizes to the pole of the cell and is thought to interact with the Type IV Pilus machinery. FimX deletion resulted in non twitching bacteria and shows defects in pilin subunit assembly and secretion. A FimX homolog in *Xanthomonas axonopodis* interacts with, PilZ another component of this machinery, where PilZ also interacts with PilB, the hexameric ATPase required for extension of pili (Guzzo et al., 2009). However, recent work has shown that this interaction is not conserved in *Pseudomonas* species (Qi et al., 2012). The domain organization of FimX is Rec-PAS-GGDEF-EAL. Interestingly, all domains

except for the PAS domain are degenerate in that they lack conserved residues required for their characteristic functions. FimX binds CDG at its C-terminal degenerate EAL domain with an affinity of 125 nM. Crystallography studies showed that the EAL domain undergoes very little conformational change (Navarro et al., 2009). However, CDG binding to the FimX EAL domain results in a long-range conformational change transmitted through the GGDEF and PAS domain to affect the conformation of the N-terminal receiver domain (Qi et al., 2011). The function of FimX binding to CDG is not known.

PelD (PA3061), one of the first non-PilZ domains shown to bind CDG is an inner membrane protein that possesses 4 transmembrane domains and cytosolic GAF and degenerate GGDEF domains. This protein is required for pel exopolysaccharide synthesis (Lee et al., 2007) and binds CDG with an affinity of 1.9 μm (Whitney et al., 2012). CDG binds to the I-site of the non-catalytically active GGDEF domain (Lee et al., 2007) and makes contact with the neighboring GAF domain. A phenotypic analysis of PelD CDG affinity mutants shows that CDG binding is required for the production of pel exopolysaccharide (Whitney et al., 2012).

Alg44 (PA3542) is a protein required for alginate production in mucoid strains and consists of an intracellular N-terminal PilZ domain, transmembrane domain, and a C-terminal periplasmic secretion family HlyD domain. This protein binds CDG with an affinity of 5.2-12.7 μM (Pultz et al., 2012) an event required for alginate production (Merighi et al., 2007).

The Role of CDG in *P. aeruginosa* Infection

CDG acts through several pathways to promote production of adhesins and exopolysaccharide needed for biofilm formation. Pel, psl, and alginate exopolysaccharides are important for biofilm formation (Friedman and Kolter, 2004a; Friedman and Kolter, 2004b) where psl is a repeating

pentasaccharide of D-mannose, D-glucose, and L-rhamnose (Byrd et al., 2009) and pel is a glucose rich polymer. Induction of pel exopolysaccharide during a biofilm model of growth provides protection against tobramycin killing. This exopolysaccharide may act as a diffusion barrier or directly bind tobramycin because of charge complementarity (Colvin et al., 2011). Alginate is another polymer consisting of β-1,4 linked D-mannuronic and L-guluronic acids (Ryder et al., 2007). Alginate hyperproducing mucoid mutants are frequently isolated in the lungs of patients with cystic fibrosis. Alg44, a PilZ domain containing protein that binds c-di-GMP is involved in the biosynthesis of alginate. CDG stimulates exopolysaccharide production by promoting transcription of pel and psl exopolysaccharide through FleQ dependent transcription (Hickman and Harwood, 2008) and exerts post-transcriptional effects *via* PelD to promote pel production (Lee et al., 2007). A positive feed-back loop was identified whereby cells increase CDG levels upon the detection of exopolysaccharide (Irie et al., 2012). CDG inhibits motility possibly in a post-translational manner by binding to the YcgR homolog (PA3353).

P. aeruginosa infection of cystic fibrosis patients is chronic and single lineages have been observed to predominate for many years. Over time, these isolates adapt to this niche by incurring mutations (Smith et al., 2006), some of which increase the propensity for forming SCVs (Kirisits et al., 2005; Häussler et al., 2003). SCVs correlate with a prolonged persistence, elevated antibiotic and serum resistance, and poor lung function (Häussler et al., 1999; Reinhardt et al., 2007). Mutations that lead to SCV formation often function to elevate CDG (Drenkard and Ausubel, 2002; Meissner et al., 2007; Starkey et al., 2009; Malone et al., 2010), therefore elevated CDG levels may provide an adaptive advantage for bacterial survival in this environment. Hyper adhesive *P. aeruginosa* biofilms are notorious in infestations of abiotic

surfaces in such as catheters and ventilators and cause significant morbidity and mortality in hospitalized patients.

Flagellar Motility

Overview

P. aeruginosa possesses a single polar flagellum, a helical polymer that rotates in two directions to either push or pull cells (Sowa and Berry, 2008). Bacterial flagellar rotation has been observed in the range of 100Hz to 1700Hz (Sowa and Berry, 2008).Counter clockwise rotation as viewed from outside of the cell is predicted to produce forward movement and clockwise rotation leads to reverse movement (Schmidt et al., 2011). The chemotaxis machinery promotes directed movement along a chemical gradient by modulating the relative frequencies of runs, reversals, and reorientations in contrast to tumbling exhibited by peritrichously flagellated bacteria (Schmidt et al., 2011). This mode of behavior is similar to that of *Vibrio alginolyticus*, where it has been shown that reorientation events are promoted by the rudder action of its single polar flagellum (Xie et al., 2011). The chemotaxis machinery controls the frequencies of runs and reversals by modulating the direction of flagellar rotation through phosphorylation of the soluble response regulator, CheY, which binds the rotor complex protein FliM in enteric bacteria.

In contrast to polarly flagellate bacteria, peritrichously flagellated bacteria exhibit directed movement by altering the frequency of runs and tumbles, where tumbling serves to randomly reorient cells (Sowa and Berry, 2008). Again, counter clockwise rotation leads to forward movement, where left handed flagella associate as a bundle. A switch to clockwise rotation initiated by phosphorylated CheY disrupts bundle formation and initiates changes in

waveform from left handed “normal” helices to right handed “curly” or “semi-coiled” helicies (Turner et al., 2000; Kim et al., 2003).

Structure of the Flagellum

The flagellum contains a motor consisting of the stator and the rotor. The cytosolic rotor is joined by a rod, hook, and multiple rings to the flagellum and the stator typically harnesses energy from proton motive force to cause the rotor, and, the flagellum, to spin. The structural core of the flagellar apparatus in gram-negative bacteria is well conserved; therefore principles learned from these studies are applicable to *P. aeruginosa* (Chen et al., 2011).The flagellar apparatus has components known as the basal body, hook, and filament (Sowa and Berry, 2008). The basal body is the core of the motor, and consists of ring structures in the cytosol, inner and outer membranes, and periplasm, known as the C-ring, MS-ring, L-ring, and P-ring, respectively. The cytosolic ring (C-ring) is the rotor switch complex component and is typically made up of three proteins, FliG, FliM, and FliN. The copy number of FliG, FliM, and FliN varies depending on the organism where the copy number of FliG and FliM can range from 23 to 36 copies and the number of FliN molecules is generally four times that of FliG (Sowa and Berry, 2008). The inner membrane ring is known as the MS ring and is made up of only the FliF protein. An inner membrane channel, termed the stator, harnesses proton motive force generated by respiration and interacts with the rotor protein, FliG, to produce torque. It is not clear how the passage of protons through the stator produces spinning of the rotor. The stator is typically composed of two transmembrane proteins termed MotA and MotB, but in *P. aeruginosa*, there are two paralogous sets of stator proteins, MotAB and MotCD. It is not clear what the individual functions of these two sets of stator proteins are. A mutant in all four genes is abrogated for swimming motility but individual mutants in *motAB* or *motCD* exhibit normal swimming motility (Toutain et al., 2005).

In contrast, each set of stator proteins is required for swarming motility as the agar concentration was increased from 0.5% to 0.8% where the requirement for *motCD* was greater than the requirement for *motAB*. The rod spans the inner and outer membrane connecting the MS ring to the hook, and is encoded by *flgBCFG*. The L-ring and P-ring are made up of *flgH* and *flgI* respectively. The export apparatus is important in flagellar assembly, as it facilitates secretion of non-cytosolic flagellar apparatus components across the inner membrane. The export apparatus consists of integral membrane proteins FlhA, FlhB, FliOPQR as well as soluble export apparatus proteins FliHIJ.

Filament Structure

The flagellar filament consists of polymerized flagellin. Individual flagellin monomers associate to form protofilaments, 11 of which then associate longitudinally to form the flagellum (O'Brien and Bennett, 1972). The protofilaments can assume either an R or an L form, and the relative composition of R and L protofilaments determines the waveform of the flagellum (Calladine et al., 2013). Waveform is used to describe the shape of the flagellum that can vary in wavelength and handedness. Twelve different waveforms have been predicted to exist based on the relative amounts of R or L protofilaments (Calladine et al., 2013), at least four of which have been observed in *E. coli* (Turner et al., 2000). Waveforms of *P. aeruginosa* flagella have not been well characterized. However, it is logical to assum that flagella form left-handed helices in order for CCW rotation to lead to forward movement. In *E. coli*, a rotor reversal from counterclockwise to clockwise rotation applies right handed torsion to the flagellum and therefore leads to a change in waveform from left to right-handed helices (Macnab and Ornston, 1977). It is not clear what the effect of rotor reversal is on *P. aeruginosa* as altering the helicity from a left to right handed helix would prevent backwards movement. Essential features of the flagellin monomer gene are

widely conserved over large evolutionary distances which led to the assumption that the flagellar structure observed in enteric bacteria and described above is a structural model for most bacterial flagella (Beatson et al., 2006). However, structural elucidation of flagellar waveforms in *Campylobacter* revealed a divergent quaternary structure indicating that the waveforms observed in *E. coli* may not occur in other bacteria such as *P. aeruginosa* (Galkin et al., 2008).

Chemotaxis Apparatus

The bacterial chemotaxis machinery functions to transduce signals from the extracellular environment facilitating movement along chemical gradients. The *P. aeruginosa* chemotaxis machinery is similar in nucleotide sequence to that of *E. coli* (they share between 32% and 58% amino acid identity) and based on phenotypes of mutant strains, the function of individual components appear to be conserved between the two organisms (Ferrández et al., 2002; Schmidt et al., 2011). The *E. coli*, chemotaxis system consists of the transmembrane methylaccepting chemoreceptors (MCPs) that control activity of an associated histidine kinase, CheA, through an adaptor protein, CheW. CheA exhibits autophosphorylation and phosphotransfer to its response regulators CheY and CheB, a phosphorelay stimulated by the absence of ligand bound to MCPs. Methylation of MCPs occurs constitutively by CheR whereas phosphorylation of CheB stimulates methylesterase activity of MCPs and is an adaptive response. Methylation increases the basal rate of kinase activation by MCPs and decreases affinity for ligand thus enabling sensitivity to ligands over a broad range of concentrations (Sourjik and Wingreen, 2012). Although only 5 chemoreceptors exist in *E. coli*, *P. aeruginosa* possesses 26 putative chemoreceptors (Ferrández et al., 2002). Chemoreceptors form arrays at the poles (Guvener et al., 2006) likely consisting of thousands of molecules. Chemoreceptors in *E. coli* form a characteristic trimer of dimers. The stoichiometry of the other components has been elucidated

such that for every six chemoreceptor dimers, there are two CheW molecules and two CheA molecules (Li and Hazelbauer, 2011). Cryo electron tomography has shown that the trimer of dimer arrangement of chemoreceptors associate to form hexagonal arrays where trimer subunits are interlinked by CheW and CheA (Briegel et al., 2012).

Interestingly, there is also a paralogous chemotaxis machinery encoded in *P. aeruginosa* called Cluster II. It is not known what the function of this chemotaxis cluster is, however it appears to not be required for flagellar mediated chemotaxis (Guvener et al., 2006). Additionally, subcellular localization studies were performed on components of Cluster I (required for chemotaxis) and Cluster II where it was determined that Cluster II components are predominantly expressed during entry into stationary phase. Furthermore, it was determined that Cluster I components are not likely to interact with Cluster II components, as fusions of CheA and cluster II CheY2 to fluorescent proteins were not observed to colocalize (Guvener et al., 2006).

Flagellar Assembly

Flagellar assembly in bacteria is highly regulated. Both 4-tiered and 3-tiered regulatory systems are utilized for transcription of flagellar components. A model of *P. aeruginosa* flagellar regulation predicts the utilization of a 4-tiered system, typical of monotrichously flagellated bacteria (Dasgupta et al., 2003). The first tier consists of the master regulator, FleQ, which acts with σ^{54}-RNA polymerase to transcribe both structural and regulatory components. The structural components include parts of the basal body, MS ring, P ring, motor, switch, export apparatus, and filament cap. Regulatory components include FleN and a two-component system FleSR. FleN exerts negative feedback on FleQ and is important for limiting flagellar number (Dasgupta and Ramphal, 2001) whereas activity of the FleRS system is required for σ^{54}-RNA

polymerase mediated expression of the remaining components of the hook basal body rod complex (HBB). In the absence of a functional HBB, the protein FlgM binds to the sigma factor FliA, rendering it non-functional. Assembly of a HBB regulates subsequent transcriptional events as the HBB facilitates secretion of FlgM, and allows FliA to initiate transcription of downstream genes including flagellin and chemotaxis machinery components. Inner membrane components include the MS-ring, made up of FliF, and some export apparatus proteins including FlhA. It was typically thought that FliF was the first component to be assembled, however recent microscopy data suggests the export apparatus protein, FlhA is the first protein to be assembled, and that some rotor proteins may be able to assemble in the absence of FliF (Li and Sourjik, 2011). The polar placement of flagella requires FlhF which is a signal recognition particle (SRP) like GTPase transcribed during the second regulatory tier of flagellar assembly (Murray et al., 2006; Schniederberend et al., 2013). The bacterial signal recognition associated GTPases, FtsY and Ffh are essential for growth and are responsible for cotranslational targeting of inner membrane and secreted proteins to the SecYEG complex. Ffh is part of the SRP whereas Ffh makes up the SRP receptor (SR). The two form a heterodimer mediating the GTP hydrolysis required for protein targeting to SecYEG. Although FlhF hydrolysis of GTP is required for wild type levels of flagellar motility, neither its GTP binding nor GTPase activity are required for polar positioning of flagella (Schniederberend et al., 2013). In all, flagellar motility is a highly regulated biological process requiring over 50 proteins for its assembly.

Objective

As demonstrated by the information provided here, efforts to elucidate the individual biological roles of CDG degradative and synthetic enzymes commonly entail the measurement of

specific phenotypes including swimming motility and biofilm formation (Kulasakara et al., 2006; Solano et al., 2009). Some mutants give seemingly redundant phenotypes, leading to questions as to why the multiplicity of enzymes exists within individual bacterial genomes. Furthermore, the extent of single cell CDG variation within a population has not been characterized.

In order to address these questions, the Miller Lab developed a genetically encoded FRET based biosensor. This biosensor allows measurement of *in vivo* CDG concentrations in the range of ~65 nM to 600 nM (Christen et al., 2010) although subsequent work in this lab has given rise to other biosensors with sensitivities centering around 3.2 μm, 4.1 μm, and 8.2 μm (Pultz et al., 2012). Use of the original biosensor revealed intracellular CDG heterogeneity within populations in *Caulobacter crescentus* and *Pseudomonas aeruginosa* (Christen et al., 2010). This thesis focuses on the effort to characterize the mechanism underlying CDG heterogeneity in *P. aeruginosa* with the goal of providing further insight into the role of individual DGCs and PDEs.

Table 1. A list of GGDEF, EAL, and HD-GYP domain containing proteins in *P. aeruginosa*

GGDEF Domain Proteins			Tandem GGDEF/EAL Domain Proteins			EAL Domain Proteins		
PAO1 locus tag	gene	function	PAO1 locus tag	gene	function	PAO1 locus tag	gene	function
PA0169	*siaD*		PA0285			PA2133		PDE
PA0290			PA0575			PA2200		PDE
PA0338		DGC	PA0861	*rbdA*	PDE	PA2818	*arr**	PDE
PA0847		DGC	PA1181			PA3825		PDE
PA1107	*roeA*	DGC	PA1433	*lapD*	receptor	PA3947	*rocR*	PDE
PA1120	*yfiN*	DGC	PA1727			(PA14)	*pvrR**	PDE
PA1851			PA2072			HD-GYP Domain Proteins		
PA2771			PA2567					
PA2870		DGC	PA3258			PAO1 locus tag	gene	function
PA3061	*pelD*	receptor	PA3311					
PA3177			PA4367	*bifA*	PDE	PA1878		
PA3343			PA4601	*morA*		PA2804		
PA3702	*wspR*	DGC	PA4959	*fimX*	receptor	PA4108		
PA4332	*sadC*	DGC	PA5017	*pac*	PDE	PA4781		
PA4396			PA5295					
PA4843			PA5442					
PA4929								
PA5487								

*Not conserved within all *P. aeruginosa* strains

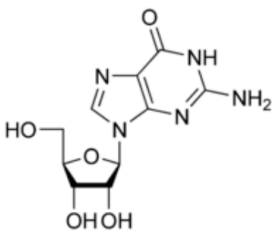

guanosine

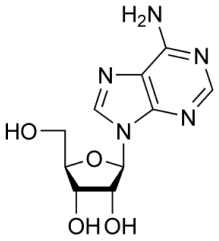

adenosine

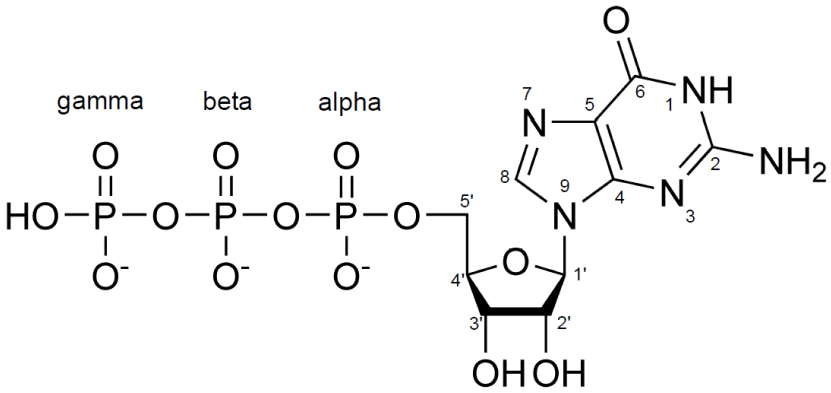

guanosine triphosphate

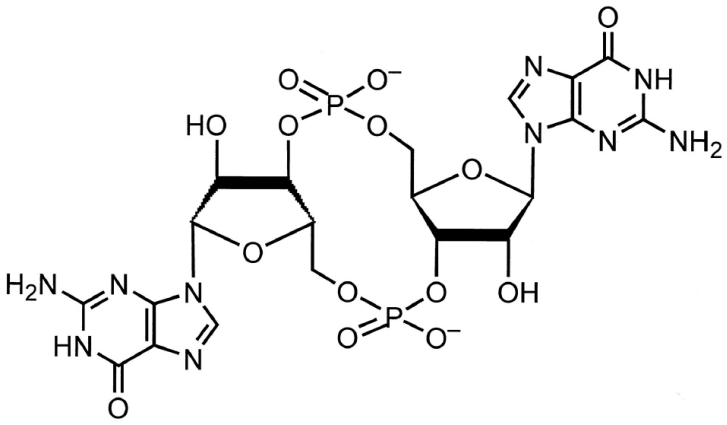

cyclic dimeric (3'->5') GMP

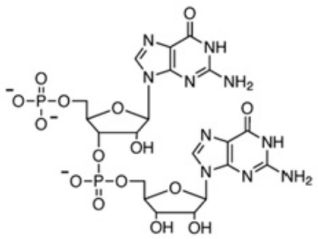

linear dimeric GMP

Figure 1. Structure of CDG and related molecules. CDG is synthesized from 2 molecules of GTP by diguanylate cyclases. Guanosine triphosphate consists of guanosine, a purine nucleoside made of guanine attached to ribose, and 3 phosphate moieties. CDG is degraded to linear dimeric GMP by phosphodiesterases.

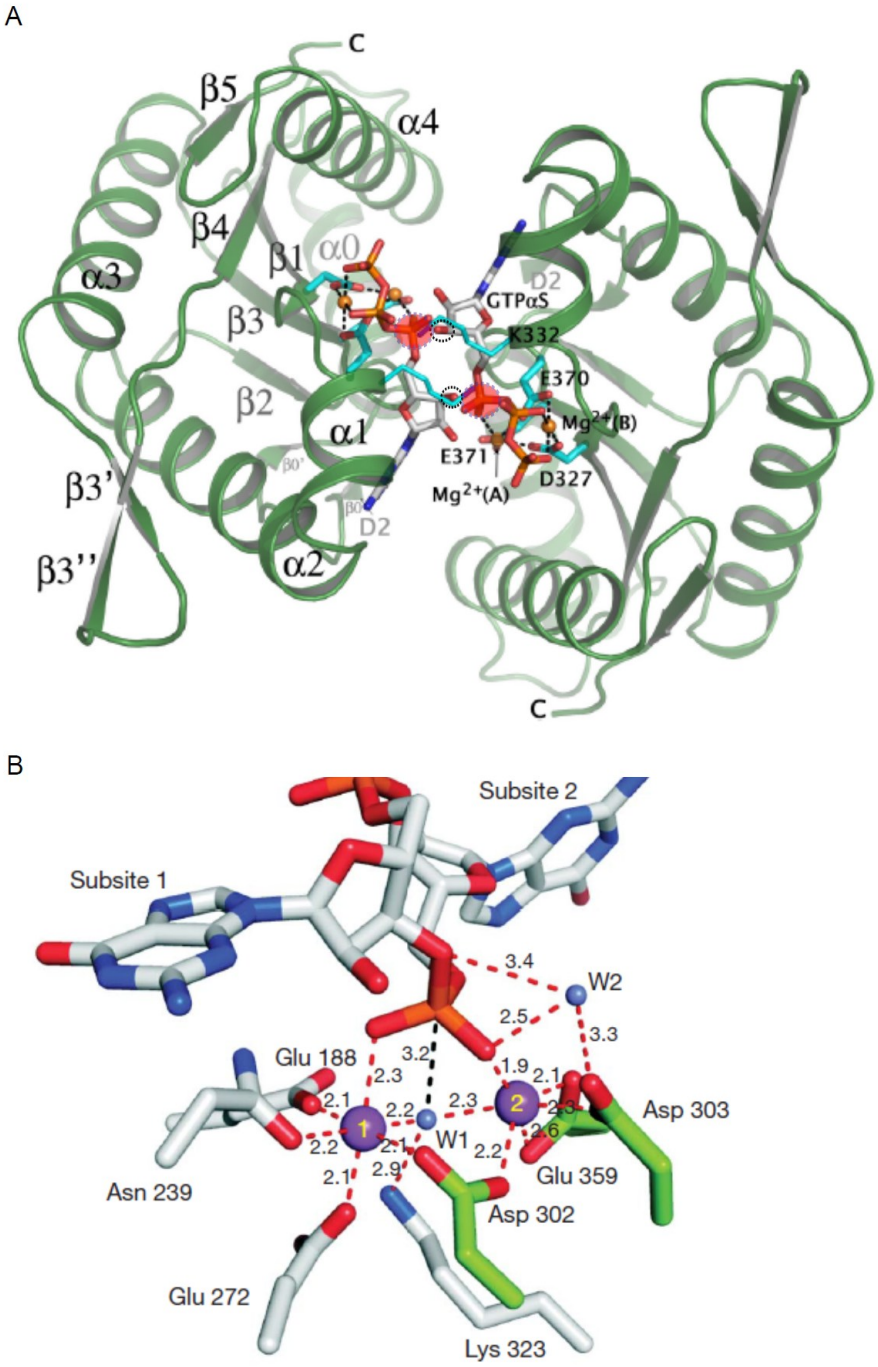

Figure 2. Proposed catalytic mechanisms. A) DGC mechanism adapted from Wassman et al. (2007). Two antiparallel GGD/EEF domains (from PleD) are in complex with GTP. The 3'OH group is deprotonated (circled in black) and initiates an intermolecular attack on the alpha phosphate (highlighted in red) of the other GTP molecule. B) Residues required for PDE catalysis. Adapted from Barends et al. (2009). W1 initiates a nucleophilic attack on the adjacent phosphorus atom. W2 donates a proton to O3 leading to its expulsion.

Chapter 2: Materials and Methods

Culture Conditions

Antibiotic concentrations used for *P. aeruginosa* strain construction were 30 μg/ml gentamycin, 150 μg/ml carbenicillin, and 25 μg/ml irgasan. Antibiotic concentrations used for maintenance of plasmids in *E. coli* were 15 μg/ml gentamicin and 100 μg/ml ampicillin. Other bacterial strains were routinely grown in LB medium. For microscopy, all strains containing a variant of pMMB67Gm were grown overnight in the presence of 100 μM IPTG and 30 μg/ml gentamicin in LB medium. The next day, cultures were diluted to 0.05 in the same medium and grown in a baffled flask with shaking at 275 rpm at 30C. For microscopy with the inducible DGC or PDE, L-arabinose was added to a final concentration of 0.2% at the time of sub-culturing. Cells were harvested at an OD600 of 0.3, pelleted, and resuspended in one fourth of the original volume in a medium formulated for microscopy because of its low intrinsic fluorescence consisting of 0.5X M63, 10mM succinate, 20mM mono potassium glutamate, 1X NEAA (Invitrogen), 2mM $MgCl_2$, and 100μM $Fe^{2+}NH_4SO_4$. 1.5 μl of this suspension was placed on a 0.75 mm thick 1% agarose pad containing the same microscopy medium and a coverslip was placed over the cell suspension before it was allowed to dry. Coverslip agarose slide sandwiches were sealed using thermoplastic glue. Amine Labeling was performed as in Skerker and Berg (2001) using Alexa Fluor 488 Carboxylic Acid, Succinimidyl Ester (Invitrogen).

Flagellar Motility Assay

Overnight cultures were diluted to an OD600 of 0.01. One µl of this suspension was spotted on motility medium consisting of 0.3% agar, 1% tryptone, and 0.5% NaCl and incubated at 30 C for ~14 hrs.

Strains and Plasmids

Initial characterization of CDG levels in *P. aeruginosa* was performed using a pyoverdine negative mutant of PA01 that has a transposon insertion in the *pvdD* gene (mutant ID 1707) (Jacobs et al., 2003). We also used mapped transposon insertions in putative DGCs and PDEs in *P. aeruginosa* strain PAO1 to screen for alterations in CDG (Jacobs et al., 2003). The effects of abrogating flagellar and chemotaxis cluster components on Pac-mCherry localization were initially determined using the two-allele collection of mapped transposon insertions (Held et al., 2012).

We used strain *P. aeruginosa* PA14 for subsequent work. In PAO1, a large population of cells that lacks detectable fluorescence is enriched over time, indicating the gene encoding the biosensor is undergoing recombination. For biosensor construction, a full-length synthetic *ycgR* allele codon optimized for expression in *C. crescentus* and *P. aeruginosa* was synthesized by GenScript (GenScript, USA). The resulting synthetic *ycgR* allele, *synthSpy* was cloned into pET15b::mYPet-12AA-mCyPet via KpnI and SpeI to yield pET15b::mYPet-synthspy-mCyPet. The pMMB67EH-based constructs for in vivo microscopy was made by PCR amplification of pET15b::mYPet-synthspy-mCyPet. The pET15b ribosomal binding site sequence was engineered immediately upstream of start codon of each construct. PCR products were cloned into pMMB67EH at EcoR1 and HindIII sites.

Deletions were constructed using the pEX18Gm allelic exchange vector and protocol outlined in (Hoang et al., 1998). Plasmids for gene deletions in *P. aeruginosa* were constructed by combining roughly 1kb fragments from upstream and downstream of the genes of interest into a suicide vector. In each instance, a primer was designed within the gene, near the 5' end and in the antisense direction, along with a corresponding primer roughly 1kb upstream in the sense direction. Similarly, a primer was designed within the gene near the 3' end in the sense direction, along with a primer roughly 1kb downstream in the antisense direction (Table 2). The two primers contained within the gene were in-frame with each other, and each contained an identical restriction site for subsequent digestion and ligation. The primers upstream of the gene in the sense direction and downstream in the antisense direction each contain unique restriction sites for cloning into the MCS of the vector. The regions upstream and downstream of the gene of interest were PCR-amplified using the Thermo Scientific Phusion High-Fidelity DNA Polymerase, and the reaction products were then purified using the Qiagen PCR Purification Kit. The purified PCR products were digested with the appropriate restriction enzymes and gel-purified for cloning using the Macherey-Nagel Nucleospin Gel and PCR clean up kit. The upstream and downstream regions were then ligated into the previously cut and gel-purified suicide vector, either pEX18Gm(Hoang et al., 1998) or pEX2 (Rietsch et al., 2005).

Strains encoding an inducible ectopic DGC or PDE contain the *C. crescentus* DGC CC3285 or PDE CC3396 at the attTn7 site with expression under the control of the pBAD promoter. To create a gene inducible system at an ectopic site in *P. aeruginosa* chromosome, we modified the pUC18TminiTn7TGm vector to include elements from pBAD18 and pJAT13 (Guzman et al., 1995; Khlebnikov et al., 2001).The genetic region containing *araC* gene, pBAD promoter, the multiple cloning site and the T1T2R5 transcriptional terminator was PCR

amplified from pBAD18. To facilitate transport of arabinose into *P. aeruginosa*, a DNA fragment containing pCP13 promoter and the *araE* gene was amplified from pJAT13-*araE*. These two fragments were ligated and cloned into Stu1-Spe1 sites in the pUC18TminiTn7TGm vector. *P. aeruginosa* does not metabolize arabinose and poorly transports it into the cell. Thus, the presence of the AraE transporter facilitates uniform transport of arabinose into every cell in the population, hence assuring gene induction in each single cell.

CheA-mTQ2 C-terminal fusion was made by fusing the *cheA* gene with the fluorophore at the 3' end using the GTGGSGGS flexible linker region and Xba1 and Kpn1 restriction sites. This fusion and roughly 1kb upstream and downstream DNA flanking the *cheA* gene was cloned into pEX18Gm vector using EcoR1 and HindIII sites. Identical strategies were used for creating the pEX18Gm derived N-terminal Flim-mKate2 fusion vector. The mKate2 gene was inserted at the 5'end of the *fliM* gene minus the start codon; again using the EAAAK(x4) linker with the same restriction sites (Table 3).

Plasmids were created to complement deletions of the *fliF*, *cheA*, and *flhF* genes in PA14 by designing primers to amplify those genes by PCR as previously described, including restriction sites at the ends of the primers (as shown in Table 4) for subsequent digestion and ligation into the pmmb67EH-GM vector (Fürste et al., 1986). The PCR, digestion, and gel-purification were all performed as previously described.

The Pac C-terminal fusion to mCherry in pUC18Tmini-Tn7T was constructed in several steps. MCherry was amplified with primers cac cat ggt acc ggc ggc agc ggc ggc agc ATG GTG AGC AAG GGC GAG G and ata tat tgt aca TTA CTT GTA CAG CTC GTC CAT GCC. The resulting product was digested with Acc65I and ligated into Acc65I digested pUC18Tmini-Tn7T. Ligating this product into the Acc65I site destroyed one site and maintained the other. The

vector that maintained the Acc65I site 5' to mCherry was used in the next step. *Pac* was amplified with cac cat gga tcc AAG TGG CGA TCC TCG GTG TGT C and ata tat ggt acc GTG CAG GGT GCG GCA GGG AT. The product was digested with BamHI and Acc651 and ligated into the vector made in the previous step. *pac* was cloned into pUC18Tmini-Tn7T using the restriction enzymes EcoRI and HindIII and was amplified using primers: cac cat gaa ttc AAG TGG CGA TCC TCG GTG TGT C and ata tat aag ctt TTA CTT GTA CAG CTC GTC CAT GCC. The E675A mutation was created by mutating codon 675 gAa to gCa in *pac* cloned into pUC18Tmini-Tn7T. Primers: TTG CTC GGC CTG GcA GCC CTG CTG CGC and GCG CAG CAG GGC TgC CAG GCC GAG CAA were used to create this mutation with a protocol outlined in the Stratagene QuickChange Mutagenesis Kit. The Pac-sYFP2 fusion plasmid was created by again using a similar strategy to that of CheA-mTQ2 fusion. The fusion construct and roughly 1000 base pairs upstream of *pac* were cloned into the BamH1-HinDIII sites of pUC18-mini-Tn7-Gm (All PCR reactions were done using the Thermo Scientific Phusion High-Fidelity DNA polymerase, and the PCR products purified with the Qiagen PCR Purification Kit. The DNA fragments for assembling fusions were digested with their corresponding restriction enzymes using Thermo-Fermentas Fast Digest enzymes and then gel-purified using the Macherey-Nagel Nucleospin Gel and PCR clean up kit. The DNA fragments were then ligated into the previously cut and gel-purified vectors using T4 DNA Ligase. All variants of *pac* were cloned to include its native promoter located in the 610 nucleotides upstream of the gene.

Microscopy Image Acquisition

Snapshot images were taken within 10-25 minutes of harvesting the cells from liquid culture. A minimum of five fields were acquired for each data set where at least three biological

replicates were collected for each data set. All images were collected in a temperature controlled chamber set to 25C. To facilitate segmentation and protein localization analyses, and to reduce possible effects on CDG from increased density, fields with a maximum of 200 cells were analyzed. Image Acquisition: Images were acquired using Nikon Elements AR software on a Nikon Ti-E (inverted) using a 100X oil CFI Plan Apochromat λ DM objective (1.45NA) and an EMCCD camera (Cascade II 1024, Photometrics) with a Xenon lamp as the light source. mCyPet (Cfp), Fret, and mYPet (Yfp) images were collected using Semrock filters and dichroics described in (Christen et al., 2010) For snapshot FRET measurements, Cfp (mCyPet) and Fret channel images were collected using 600ms exposure times with 2x2 binning and a multiplier of 3035. Yfp (mYPet) images were collected using 100ms exposure with 2x2 binning and the same multiplier. For timelapse imaging, exposure times for Cfp and Fret images were reduced to 300ms and the Yfp image was omitted to reduce photobleaching. mCherry2 and mKate2 fluorescence were collected using a filter cube designed for mCherry fluorescence (mCherry-40LP-A-000-ZERO, Semrock) with an exposure time of 1s and 2x2 binning and mTurquoise and SYFP2 were imaged using the filter set used for Cfp and Yfp, respectively. For both, 1x1 binning and exposure times of 600ms and 1.2 s were used.

Microscopy Image Analysis

Cell segmentation and fluorescence intensity analyses were performed using custom written Matlab software that was used previously for analysis of bacterial single cell microscopy data in LeRoux et al. (2012) and O'Connor et al. (2012). Prior to analysis in Matlab, images for the measurement of biosensor activity were preprocessed in ImageJ. To correct sub-pixel registration defects both Cfp and Yfp images were aligned to the Fret image using the Plugin

TurboReg (Thevenaz et al. 1998) and background was subtracted using the rolling ball subtract background menu option. In Matlab phase contrast images were used for automated segmentation (LeRoux et al., 2012), (O'Connor et al., 2012) The segmentation defined the boundaries of individual cells used in all analyses of fluorescence intensities. Cells not expressing the biosensor (less than 5% of cells) were excluded from the analysis by removing cells with Yfp average arbitrary fluorescence units of less than 1500. Here, net Fret (nFret) is defined as the average Fret intensity minus the average Cfp intensity multiplied by the spectral bleedthrough coefficient for Cfp into the Fret channel. This was calculated for these exposure conditions for cells expressing mCyPet alone to be 0.46. The original nFret equation subtracts bleedthrough from Yfp into the Fret channel as well (Xia and Liu, 2001). Because imaging mYPet significantly increases photobleaching over time, our calculation of nFret does not include subtracting Yfp from the Fret signal. Polar intensity was defined as the area residing within either end of the cell along the long axis within one fourth of the length of the cell. Individual fluorescent foci were identified using a watershed-based segmentation algorithm and fit using a Gaussian point-spread function. A score was assigned to each focus proportional to the ratio of the peak intensity value to the standard deviation of the fit function. Polar localization was defined by locus intensity score and proximity to the pole.

Biosensor Activity Calibration to CDG Concentrations

The binding curve of the CDG biosensor in response to ligand was determined in Christen et al. (2010) and exhibits a Hill coefficient of 2 and a K_d of 198 nM at 25C. It was previously verified that fret from purified biosensor as measured by microscopy gives a dose-response binding curve similar to that as measured by a plate reader instrument. Levels of fret as

measured by microscopy corresponding to saturated or unsaturated biosensor were determined by measuring biosensor activity in cells expressing the ectopic DGC or PDE (Figure 3). Points in between were interpolated using the binding curve mentioned above. To minimize error, only points between 10% and 90% saturation are marked on the scale. For a more in depth discussion of the calibration of biosensors, refer to (Bermejo et al., 2011).

Photobleaching Correction

To correct for photobleaching that occurs during timelapse imaging, the Cfp and FRET channel images were multiplied by a correction factor that was determined by dividing the average cellular fluorescence of cells in that channel by the average cellular fluorescence at time zero. Fluorophores mYPet and mCyPet exhibit different photobleaching curves, meaning that the amount of FRET influences the rate at which bleaching occurs. Therefore we determined bleaching correction factors by dividing the populations of cells into those that exhibit high or low fret and took the average of these two numbers to prevent any bias in apparent bleaching that would occur because of disparate numbers of cells exhibiting high and low FRET.

Table 2: Primers for creating gene deletions

Name	Sequence
cheBUSSEco	CACCAAGAATTCGCTGGTGGGCGAAGAGAC
cheBUSASXba	ATATATTCTAGATCACACCAGGACTTTGACTGCCAT
cheBDSSXba	ATATATTCTAGAGGGCTCGACGACATCGG
cheBDSASH3	AATAATAAGCTTGAGCGGTCGGGCTGGTTG
cheRUSSEco	CACCAAGAATTCACGACCGTCTGAGGGGAG
cheRUSASXba	ATATATTCTAGATCACGCATTAGCTGCCGACAC
cheRDSSXba	GCGTGATCTAGACTGCCCGACCACTACCAG
cheRDSASH3	TATATAAAGCTTGGAGAGGAAGTCGTCGC
fliGUSSKpn	CACCAAGGTACCGCTGGACAAGTCGCAGGTCACC
fliGUSASNdeXba	ACTCATTCTAGAATATATCATATGGGCGCTTACTCATCGGCGTT
fliGDSSXba	ATATATTCTAGAATGAGTGAGAATCGTCTCGCCGCC
fliGDSASH3	AATAATAAGCTTATCAGTTCGCTGGGATTGTCTTTGT
fliMUSSEco	CACCAAGAATTCTGACCTTCGCCAGTCCCAACG
fliMUSASNdeXba	GGCCATTCTAGAATATATCATATGGGGATACCTACTGCAGCACGAAATTG
fliMDSSXba	ATATATTCTAGAATGGCCGTGCAAGATCTGCTTT
fliMDSASH3	AATAATAAGCTTGCCTGTTCCTCGGTGGTCACTT
fliFDSSXba	tatataTCTAGATTAATTTGAATCCTGCAACCTGTGCTGGGC
fliFUSASXba	AATTAATCTAGAAACCTGGCTGTCGATCAGTGCATC
fliFUSSSacI	CACCAAGAGCTCCACAGCCGCAAGATGAACCTCG
fliFDSASH3	cacacaaagcttCTGCGAGTAGAACGGAATGCTGTC
flhFUSSEco	CACCAAGAATTCGGGCTGGGACGATGTCAC
flhFUSASXba	GTAGAGTCTAGAGGCGGCGAAGAAGCGT
flhFDSSXba	GCCGCCTCTAGACTCTACCAGCAACCGGCG
flhFDSASH3	ATATATAAGCTTGGGGTGTTGGACCAGTCGTT
cheYUSSKpn	CACCAAGGTACCAGTATGTAGGTGTCATCCCTTACG
cheYUSASNew	CTCTCATCTAGACATCGTGGAAAAGTCGTCCAC
cheYDSSNew	ATATATTCTAGATGAGAGCGGGTCAACGGCTGA
cheYDSASH3	ATATATAAGCTTCATTCGGCTGCTCCCAGA
cheAUSSBam	CACCAAGGATCCGCTTGGTAACGATTCCACGGG
cheAUSASXba	TCCCAATCTAGAGCCCTTGACCGTATGGAACC
cheADSSXba	AAGGGTTCTAGAGTGGGACAAGAAGAAGTGGTGA
cheADSASH3	ATATATAAGCTTCCGCCAGAACCTTGTCGTT
bdlAUSSEco	CACCAAGAATTCCTACCTCTGGCAGGAAATGG
bdlAUSASXba	GTGCGTTCTAGACATGGAGCGGTCCAGCG
bdlADSSXba	TCCATGTCTAGAACGCACAAGGTGGTGGAG
bdlADSASH3	AATTAAAAGCTTAACTAACGGCGAAGCGGC

Table 3: Primers for creating gene fusions (restriction sites underlined)

Name	Sequence
5017fusSBam	caccaaGGATCCAAGTGGCGATCCTCGGTG
5017fusligAS	AATATTGGTACCGTGCAGGGTGC
linkerYFP_SKpn	ATATATGGTACCGGGGGCAGCGGCGGCAGCGTGAGCAAGGGCGAGGAG
YFP_ASH3Stu	TAATAAGGCCTATATATAAGCTTTCACTTGTACAGCTCGTCCATGC
cheAfusUSSEco	CACCAAGAATTCCACGGCAAGGGCAAGTTCA
cheAfusUSASKpn1	ATATATGGTACCGATGCGCCGTGCGTAAC
cheAfusDSSXba	ATATATTCTAGACGCCGCGTATGGGTTTC
cheAfusDSASH3	ATATATAAGCTTCCGCCAGAACCTTGTCGTT
linker_mTQ2Kpn1	ATATATGGTACCGGCGGCAGCGGCGGATCCGTCAGCAAGGGCGAGGAGCT
mTQ2ASXba	ATATATTCTAGATTACTTGTACAGCTCGTCCATGCC
FliMUSSEco	CACCAAGAATTCTGACCTTCGCCAGTCCCAACG
FliMUSASNdeXba	GGCCATTCTAGAATATATCATATGGGGATACCTACTGCAGCACGAAATTG
FliMDSSXba	ATATATTCTAGAATGGCCGTGCAAGATCTGCTTT
FliMDSASH3	AATAATAAGCTTGCCTGTTCCTCGGTGGTCACTT
altHL4ASXba	TATATATCTAGACGCCGCGGCTTTTGCTGCAGCTTCTTTCGC

Table 4: Primers for creating complementation plasmids (restriction sites underlined)

Name	Sequence
cheAUSSEco	CACCAAGAATTCATCGCTGCCGTTAAGTAAGC
cheADSASH3	ATATATAAGCTTCATAGCTACTCCTCAGAGG
flhFUSSEco	CACCAAGAATTCGGGGCAGAACTGAACGAG
flhFDSASH3	ATATATAAGCTTCGCTTCCGTCACCCG
fliFUSSKpn1	CACCAAGGTACCAGATGCCGGTCTGAGCG
fliFDSASH3	ATATATAAGCTTGCGAGACGATTCTCACTCATG

Table 5: List of Strains

Strain	genotype	locus tag
BCH001	*Δpac*	PA5017
BCH002	*Δpac attTn7::pac*	
BCH003	*Δpac attTn7::pacE675A*	
BCH004	*Δpac attTn7::pac-mcherry*	
BCH005	*Δpac attTn7::pac-syfp2*	
BCH006	*fliM-mkate2*	PA1443
BCH007	*flhF*	PA1453
BCH008	*fliF*	PA1101
BCH009	*cheA*	PA1458
BCH010	*cheY*	PA1456
BCH011	*cheB*	PA1459
BCH012	*cheR*	PA3348
BCH013	*cheAH49N*	
BCH014	*Δpac attTn7::pac-mcherry fliF*	
BCH015	*Δpac attTn7::pac-mcherry flhF*	
BCH016	*Δpac attTn7::pac-mcherry cheA*	
BCH017	*Δpac attTn7::pac-mcherry cheY*	
BCH018	*Δpac attTn7::pac-mcherry cheB*	
BCH019	*Δpac attTn7::pac-mcherry cheR*	
BCH020	*Δpac attTn7::pac-mcherry cheAH49N*	
BCH021	*Δpac attTn7::pac-mcherry ΔcheA*	
BCH022	*cheA-mTurquoise*	
BCH023	*Δpac attTn7::pac-mcherry cheA-mturquoise*	
BCH024	*Δpac attTn7::pac-mcherry cheA-mturquoise ΔflhF*	
BCH025	*fliM-mkate2 cheA-mturquoise*	

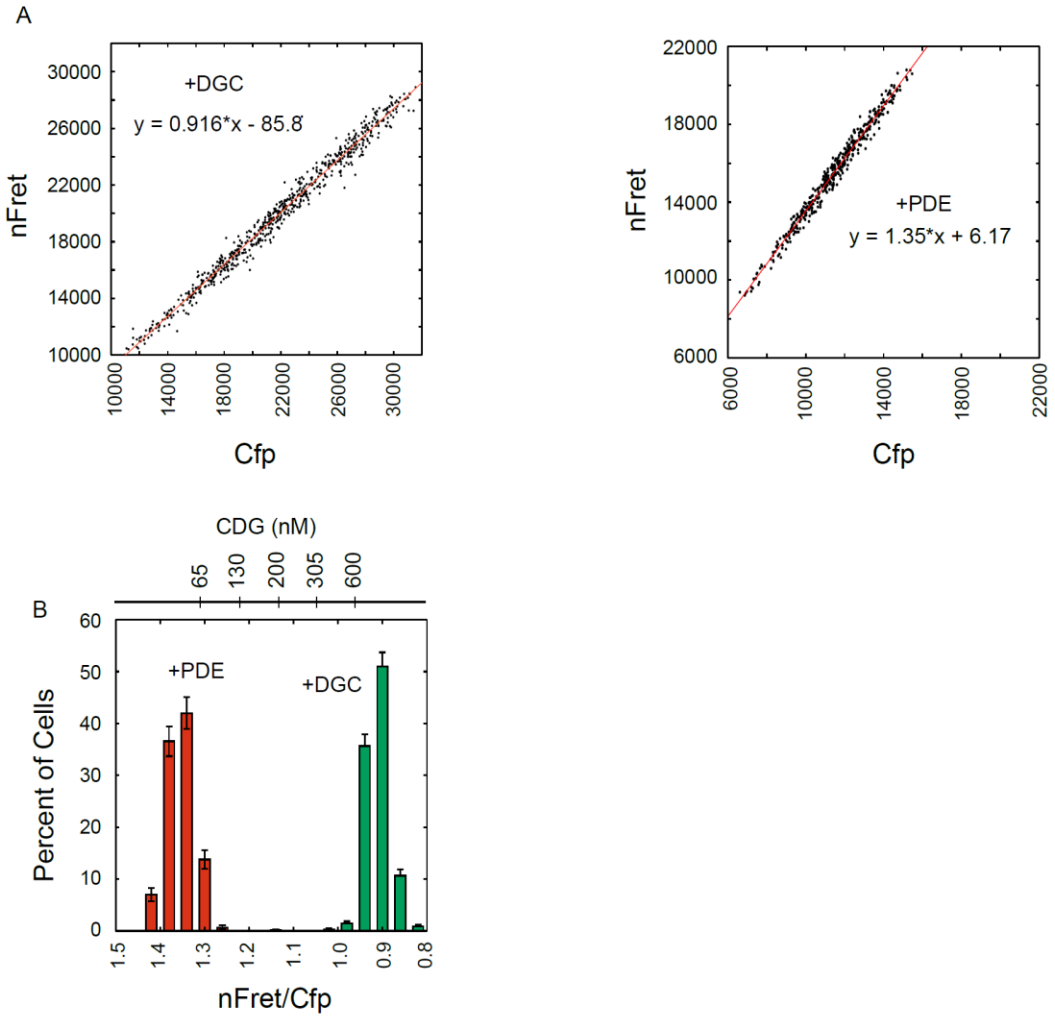

Figure 3. Calibration of biosensor activity to CDG concentration. A) Shown are scatterplots of cellular nFret vs. Cfp for strains expressing an ectopic DGC on the left and PDE on the right. B) Histograms of nFret/Cfp values per cell where the values for the DGC strain are depicted in green and PDE are depicted in red. Error bars depict counting error. The nFret/Cfp ratios of 0.916 and 1.35 were used to represent completely unsaturated and saturated biosensor, respectively. The derived CDG scale is shown above.

Chapter 3: CDG is Distributed Asymmetrically in *P. aeruginosa*

Background: Development of a Novel Biosensor Reveals CDG is Distributed Asymmetrically in *C. crescentus*.

In 2010, the Miller Laboratory developed a genetically encoded FRET-based biosensor utilizing the *S. typhimurium* CDG binding protein YcgR (Christen et al., 2010) (Figure 4). This permits measurement of intracellular CDG concentrations within single cells, in real time, and enables characterization of temporal CDG fluctuations and the resulting bacterial population heterogeneity. The biosensor was used to characterize temporal and spatial CDG fluctuations in the bacterium *Caulobacter crescentus* (Figure 5A) (Christen et al., 2010). *C. crescentus* has asymmetric cell division, resulting in two morphologically distinct progeny: a surface-attached replication-competent stalk cell, and a motile swarmer cell with a polar flagellum. The flagellated cell was found to exhibit a cytosolic c-di-GMP concentration below 100 nM and the stalked cell exhibited a concentration above 500 nM (Figure 5A and 5B). Thus, CDG is asymmetrically distributed in *C. crescentus* immediately after cell division, with low apparent levels in the flagellated swarmer cell and levels at least five times greater levels in the non-motile stalked cell.

A Biosensor Reveals CDG is Distributed Asymmetrically in *P. aeruginosa*

Like *C. crescentus*, *P. aeruginosa* produces a single polar flagellum that is partitioned to one daughter at cell division and can be visualized microscopically by labeling living cells with Alexa Fluor 594 conjugated to surface amine–specific succinimidyl ester (Fig. 5C). Before cell division, two cell poles were found to harbor similar c-di-GMP levels, probably because of rapid

diffusion of the second-messenger molecule. When septum formation resulted in two distinct cells, c-di-GMP rose above 500 nM in the nonflagellated daughter cell and dropped in the flagellated cell below 100 nM (Figure 5C). This asymmetrical second-messenger distribution was not a stochastic event: lower CDG levels were always found in the flagellated cell rather than the nonflagellated one (Figure 5D).

Flagellar Assembly Occurs at the New Pole

To identify the pole where flagellar assembly occurs, an N-terminal fusion of the rotor protein FliM to mKate2 was constructed in place of native *fliM*. This FliM-mKate2 fusion strain exhibited swimming motility (Figure 6A), and flagella labeled using amine specific Alexa Fluor 488 showed that FliM-mKate2 foci correspond to the native position of the flagellum (Figure 6B). As expected, the daughter cell that exhibited lower CDG possessed a FliM-mKate2 focus at its incipient cell pole (Figure 6C). The flagellum is inherited by one cell and is therefore preferentially synthesized in only one daughter cell prior to the next round of cell division (Suzuki and Iino, 1980). Timelapse microscopy of FliM-mKate2 indicated that flagella are assembled at the new poles (Figure 7A) as suggested by previous data (Suzuki and Iino, 1980). In the two daughter cells, the inherited flagellum marks the site of the old pole whereas the newly synthesized flagellum marks the site of the new pole until cell division (Figure 7B).

A Functional Flagellar Secretion Apparatus but not Polar Flagellum is Required for Maintenance of Low CDG

A drop in CDG is associated with the flagellum or other proteins assembled only at the new pole suggesting maintenance of low CDG may require an intact flagellum. To test this hypothesis,

CDG was measured in a strain lacking *fliF*, an inner membrane component of the MS-ring. This protein is one of the first components of the flagellum to be assembled in organisms with a homologous *fliF* gene (Li and Sourjik, 2011), and the presence of *fliF* is required for *P. aeruginosa* assembly of a functional flagellum (Arora et al., 1996). Whereas 20% of wild type cells exhibit CDG levels less than 200 nM, the *fliF* mutant exclusively exhibited CDG levels greater than 200nM (0.1% have < 200nM CDG) indicating that a flagellar component or intact flagellum is required for the maintenance of low CDG (Figure 8A).

We also measured the effect of deleting *flhF* on CDG. This protein is a signal recognition particle (SRP) GTPase required for polar positioning of the flagellum and when deleted, the position of the flagellum is not restricted to the pole (Murray et al., 2006). In an *flhF* deletion, biosensor activity shows that cells are still able to maintain low CDG levels indicating that maintenance of low CDG does not require polar flagella (Figure 8B).

A Deletion in the MS-ring Component, *fliF,* Does not Abrogate FliM-mKate2 Foci Formation

Historically, *fliF* has been reported to be the first flagellar component to be assembled. However, recently, it was reported that export platform proteins are actually assembled prior to FliF, and that the export platform proteins may facilitate rotor protein assembly in the absence of FliF. Therefore, we measured the effect of a *fliF* deletion on FliM-mKate2 localization. As in *E. coli*, FliM-mKate2 localization to the pole was not dependent upon *fliF* (Figure 8C). Unexpectedly, localization appeared to be increased relative to that of wild type and was often found to be at both poles, in addition to the septum.

P. aeruginosa Flagella Exhibit Multiple Waveforms

In the process of identifying flagellar structures in the FliM-mKate2 strain, we were able to monitor flagella in motile and nonmotile cells. It is a logical assumption that flagella form a left-handed helical structure while rotating as current work indicates counter clockwise rotation leads to forward movement in *P. aeruginosa* (Schmidt et al., 2011). As expected, flagella assuming left handed helices were observed for many motile cells (Figure 9). In peritrichously flagellated, enteric bacteria, polymorphic transformations of waveform are observed concordant with cell tumbling and are caused by right handed torsion applied from the clockwise motor rotation (rotation in the opposite direction) (Macnab and Ornston, 1977; Turner et al., 2010). We observed very few cells reversing in direction, perhaps because we monitored cells undergoing near surface motility where external forces differ from those exerted on cells during non-surface associated motility (Conrad, 2012).

Furthermore, left handed helices of rotating flagella in both stationary cells and motile cells were different from those exhibited by stationary flagella in that the pitch of the waveform was larger (Figure 10) (Figure 9). Polymorphic transformations from left to right handed helices (Figure 10) were also observed in stationary cells and occasionally motile cells. In general, the long axis of the flagellum was parallel to the long axis of the cell. The right handed helical flagella were notable in that their long axes were not perpendicular to the long axis of the cell body. *Vibrio alginolyticus* flagella have been observed to act as rudders to reorient cells during motility. It is possible that rudder action also occurs in *P. aeruginosa* where transition to the right handed waveform could be a mechanism for rudder formation (Xie et al., 2011).

Discussion

In *C. crescentus* distinct CDG levels were known to be required for cell differentiation and thus, this result confirmed the temporal nature of CDG. *C. crescentus* exhibits an asymmetric cell cycle because the two daughter cells have unique morphologies as well as functions in terms of motility and ability to undergo cell division (Tsokos and Laub, 2012). The asymmetrically differentiated daughter cells are known as the swarmer and stalked cells, where the swarmer cell carries a flagellum and pili enabling motility and the stalked cell carries an appendage that enables attachment to abiotic surfaces. Only stalked cells are competent to immediately undergo cell division. In order to divide, swarmer cells undergo morphogenesis, shedding the flagellum and pili and facilitate chromosome replication by degrading the replication repressor, CtrA (Quon et al., 1998). The FRET based biosensor showed that the CDG level was less than 100nM in the swarmer cell but then rose to a level greater than 500 nM during the swarmer to stalked cell transition. Previous observations had concluded that lower CDG is required in the swarmer cell to promote motility and higher CDG is required during morphogenesis to initiate chromosome replication. Specifically, high levels of CDG are required in the stalked cell to promote degradation of the protein CtrA which occurs when CDG binds the effector PopA with an affinity of 2 μM (Duerig et al., 2009). Low CDG promotes motility, as CDG binding to DgrA, the YcgR homolog, inhibits swimming motility (Christen et al., 2007). In *E. coli* and *S. typhimurium*, flagellar motors turn in a counter-clockwise direction as viewed from the outside of the cell to cause forward motility. The DgrA homolog, YcgR, inhibits swimming motility and chemotactic behavior in these organisms by promoting CCW rotation leading to smooth swimming and disengaging the flagellar rotor from the stators (Paul et al., 2010; Fang and Gomelsky, 2010; Boehm et al., 2010).

With the exception of the single polar flagellum, *P. aeruginosa* does not exhibit an asymmetric cell cycle because the two daughter cells are morphologically similar, and both exhibit similar capacities for undergoing cell division. Unlike in *C. caulobacter*, there had not been prior evidence alluding to the dynamic nature of CDG levels in *P. aeruginosa*, and thus the role of asymmetric distribution of CDG in *P. aeruginosa* was unexpected. It is likely that the function of this differential level of CDG in the flagellated cell is similar to that in *C. crescentus* of promoting flagellar motility. It is known in *P. aeruginosa* that increased levels of CDG inhibit swimming motility (Li et al., 2007), and a homolog of YcgR is encoded in the *P. aeruginosa* (PA3353) genome, suggesting this specific mode of regulation is preserved. However, it also seems likely that asymmetric distribution of CDG has alternate functions in *P. aeruginosa* as indicated by the variety of receptors for this molecule (Christen et al., 2010), (Pultz et al., 2012).

We determined flagella are synthesized at the new pole and therefore reasoned that a drop in CDG is not associated with a polar identity, but with proteins synthesized and retained at the new pole. Therefore, this suggested the flagellar organelle may be required for generating a drop in CDG. We tested this hypothesis and found that flagella, but not polar placement is required for maintenance of low CDG levels.

Why would the flagellum be required for maintenance of low CDG? Structural components of this organelle may inhibit DGC activity or stimulate PDE activity. Alternatively, this organelle may be required because a functional hook basal body and rod complex mediate secretion of the anti-sigma factor FlgM that renders FliA free to initiate transcription of several chemotaxis genes. Therefore, chemotaxis proteins may be involved in regulating CDG levels as opposed to flagellar genes. Identification and of the enzymes involved in generating heterogeneity in CDG levels, characterizing their localization patterns, and determining whether

they are dependent upon the flagellar or the chemotaxis complex will provide more insight as to which complex contributes to CDG heterogeneity.

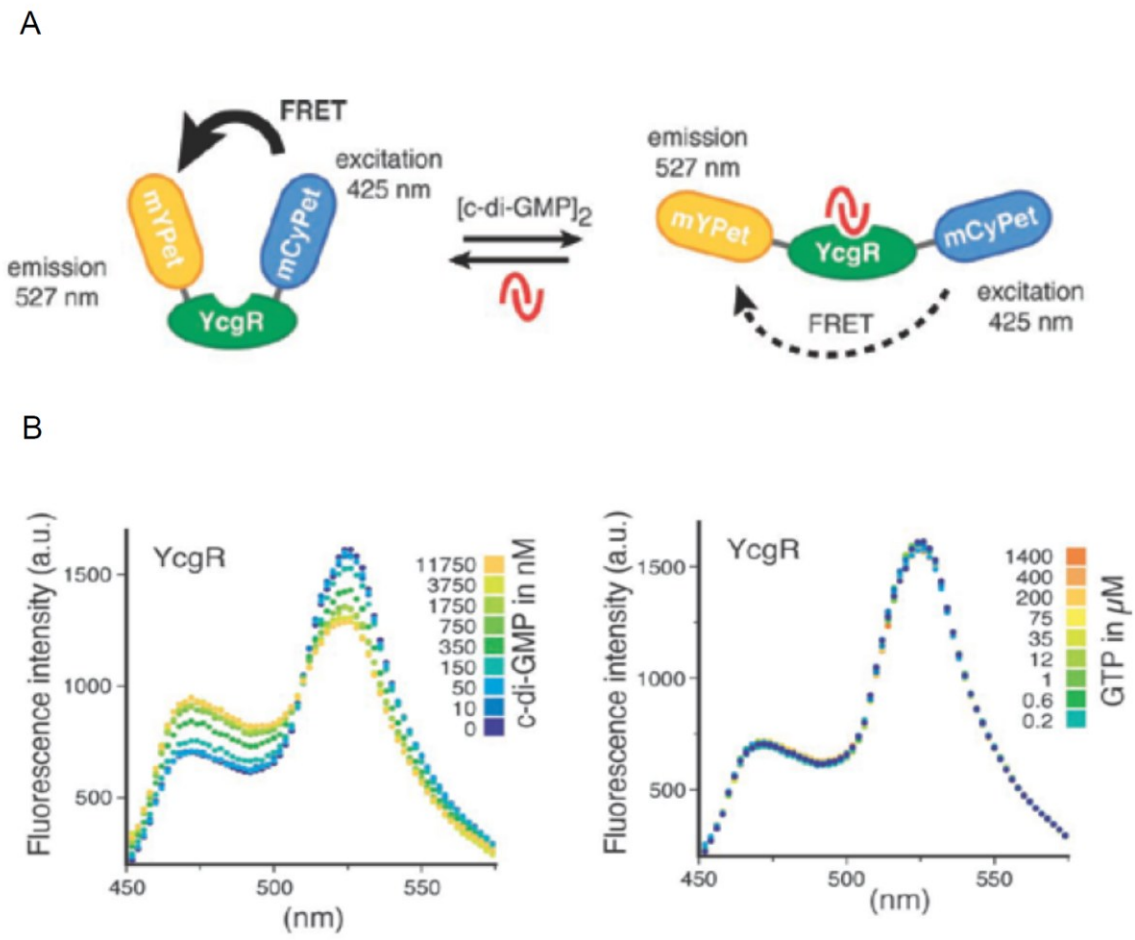

Figure 4. The CDG biosensor A) A schematic of the FRET based CDG biosensor in the presence and absence of ligand. B) Scanning emission curve of biosensor in the presence of various amounts of CDG (left) and GTP (right). Both panels are adapted from Christen et al. (2010)

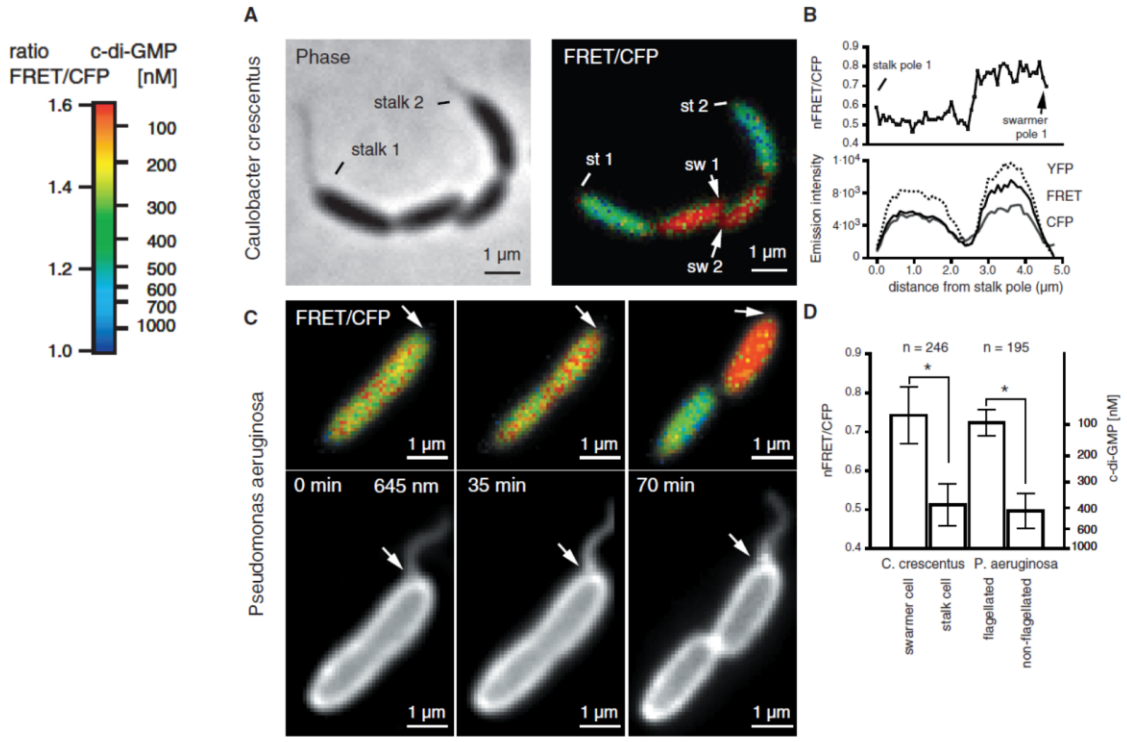

Figure 5. Asymmetrical distribution of CDG occurs following cell division. A) Phase-contrast (left) and pseudocolored FRET/CFP (right) images of dividing *C. crescentus* cells reveal CDG distribution between stalk and swarmer progeny cells. Colors represent differences in CDG concentration as indicated by the legend at left. Lines label the stalk poles (st), and arrows mark flagellated and swarmer poles. *Caulobacter* stalk cells had CDG levels above 500nM, whereas levels were below 100 nM in the swarmer cell. B) Profile of the ratio of nFret to CFP emission fluorescence (top) and (bottom) emission intensity, along the stalk-swarmer polar cell axis of the dividing *Caulobacter* cell no. 1 from A). C) CDG polarization in a dividing *P. aeruginosa* cell. Dual-emission ratio microscopic images (FRET/CFP). Surface exposed amine groups have been stained with Alexa Fluor 594; arrows indicate the position of the polar flagellum. D) Mean nFRET/Cfp ratios for flagellated and nonflagellated *Caulobacter* and *Pseudomonas* cells as indicated. Results shown are averages of single-cell measurements from at least three fields +/- SD.

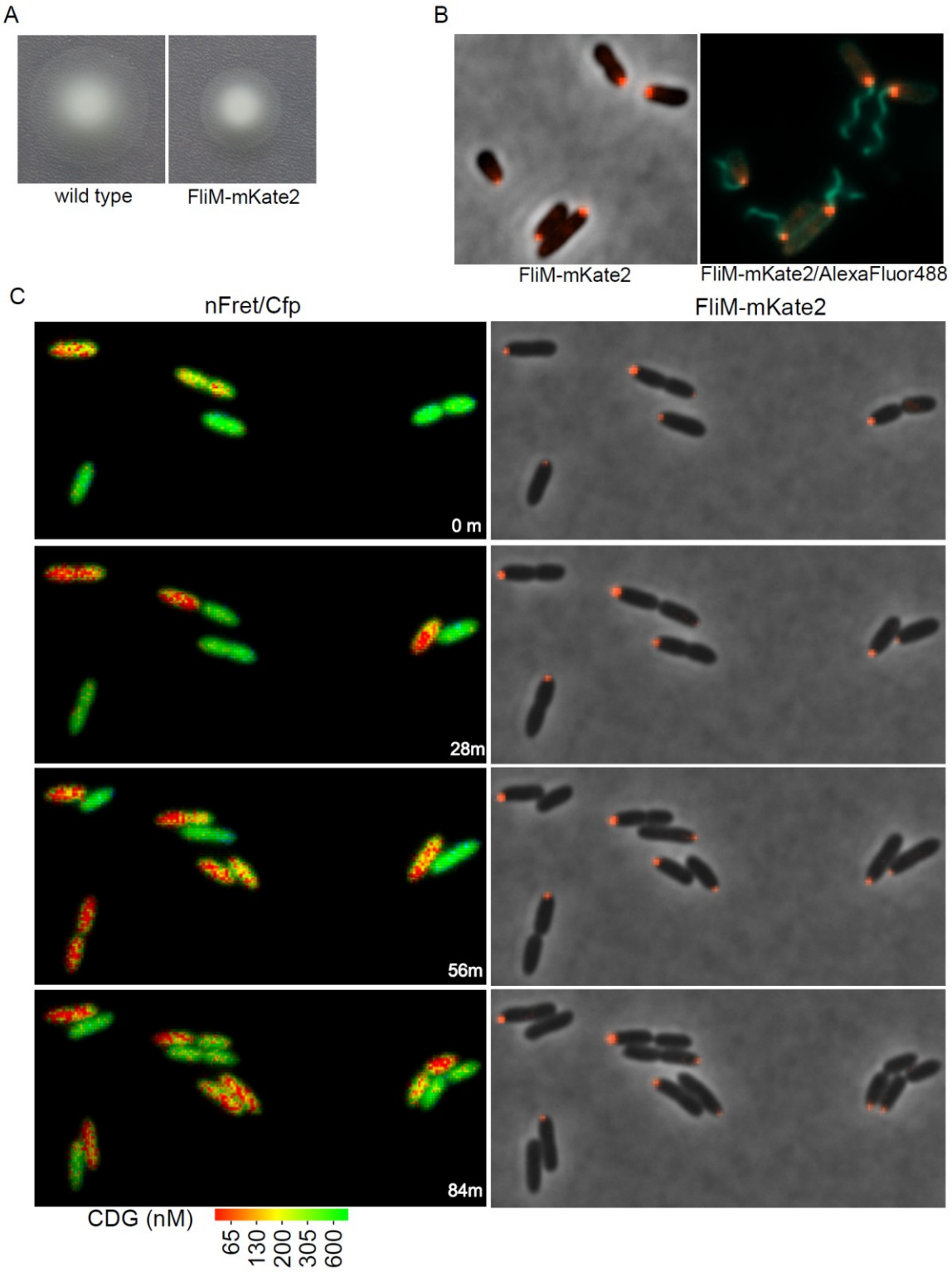

Figure 6. FliM-mKate2 characteristics. A) Swimming motility of the FliM-mKate2 fustion strain compare to wild type. B) FliM-mKate2 localization together with AF488 labeling of surface exposed amine groups. The left panel shows the overlay of FliM-mKate2 (in red) with the phase contrast image. The right panel shows FliM-mKate2 and amine labeled cells (in green). C) FliM-mKate2 localization and CDG levels over time.

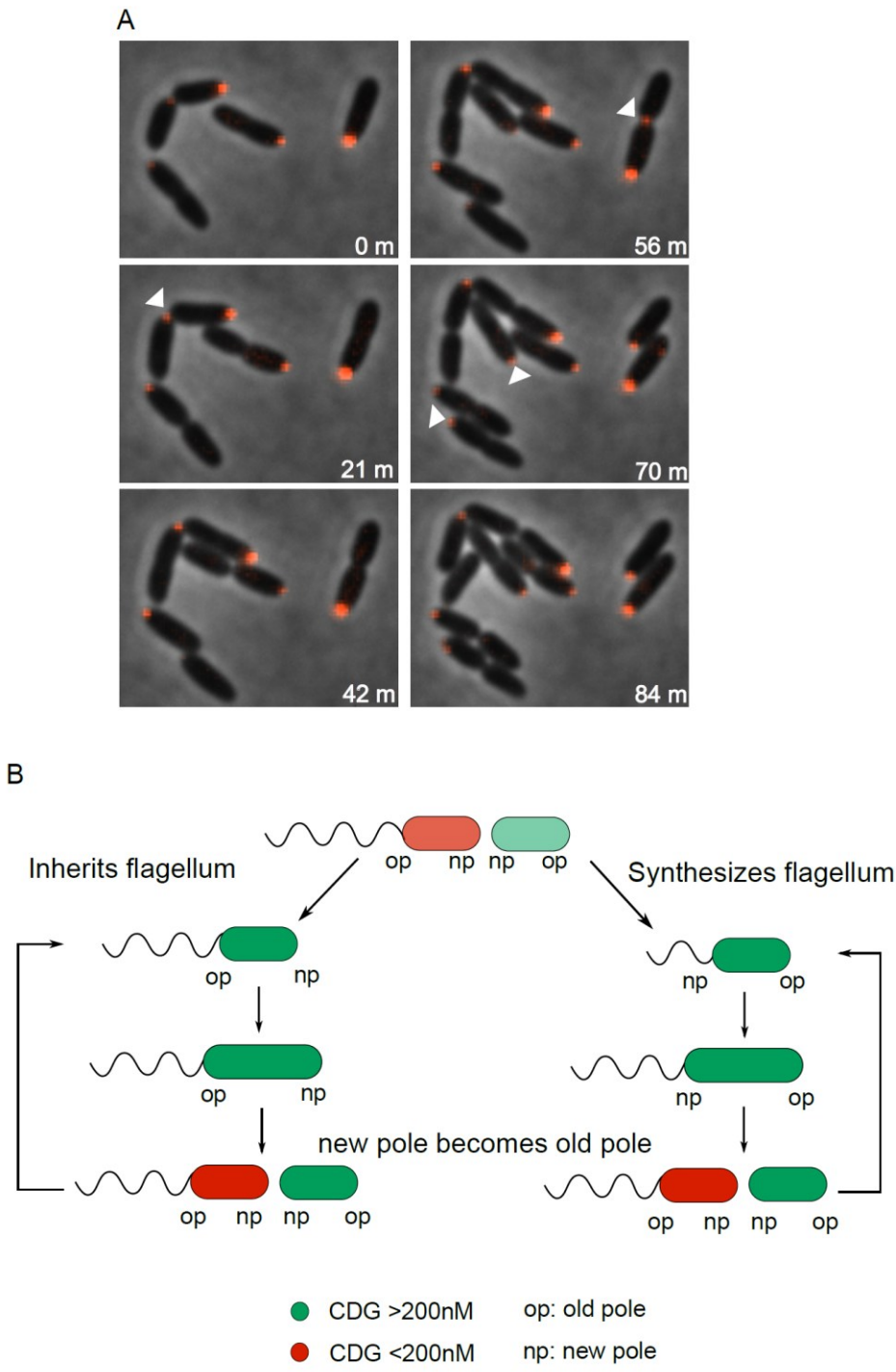

Figure 7. Flagellar assembly as related to CDG levels. A) Using FliM-mKate2 as a marker of flagellar assembly reveals flagella are assembled at the new pole. B) An illustration of flagellar assembly and CDG levels in cells of different lineages.

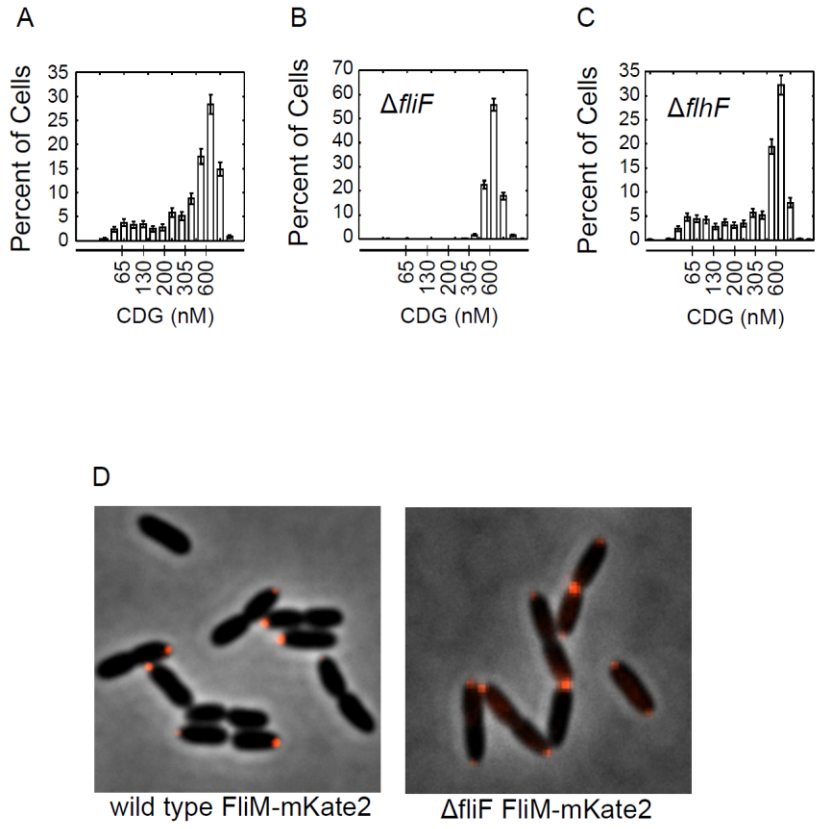

Figure 8. The effect of flagellar mutants on CDG levels and FliM-mKate2 assembly. A) CDG levels in wild type cells. B) CDG in an MS-ring mutant. C) CDG levels in an *flhF* mutant. D) FliM-mKate2 assembly in wild type and *fliF* mutant cells.

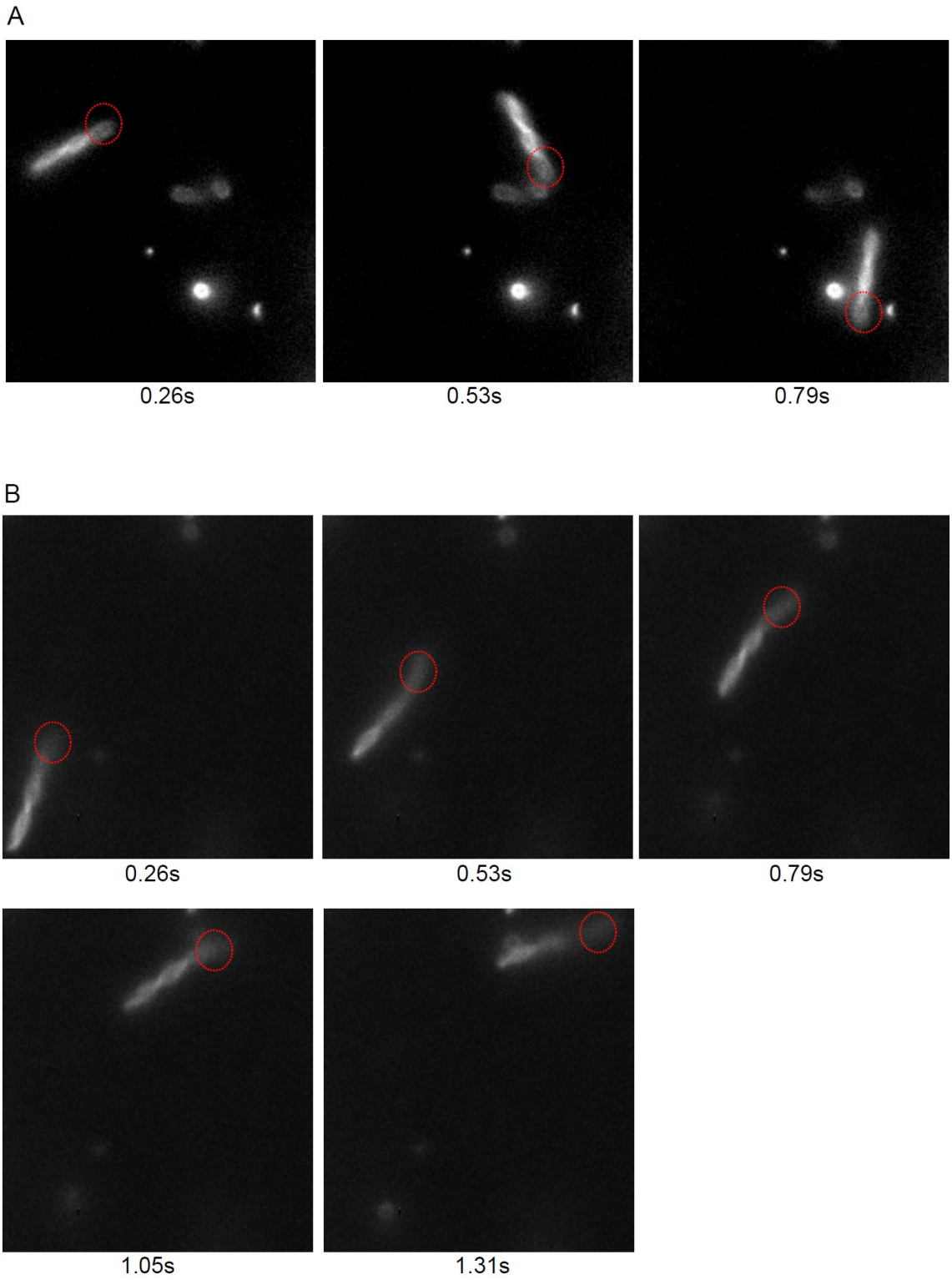

Figure 9. Flagellar waveforms exhibited by motile bacteria. A) and B) are time series from two different cells. The cell body has been circled in red.

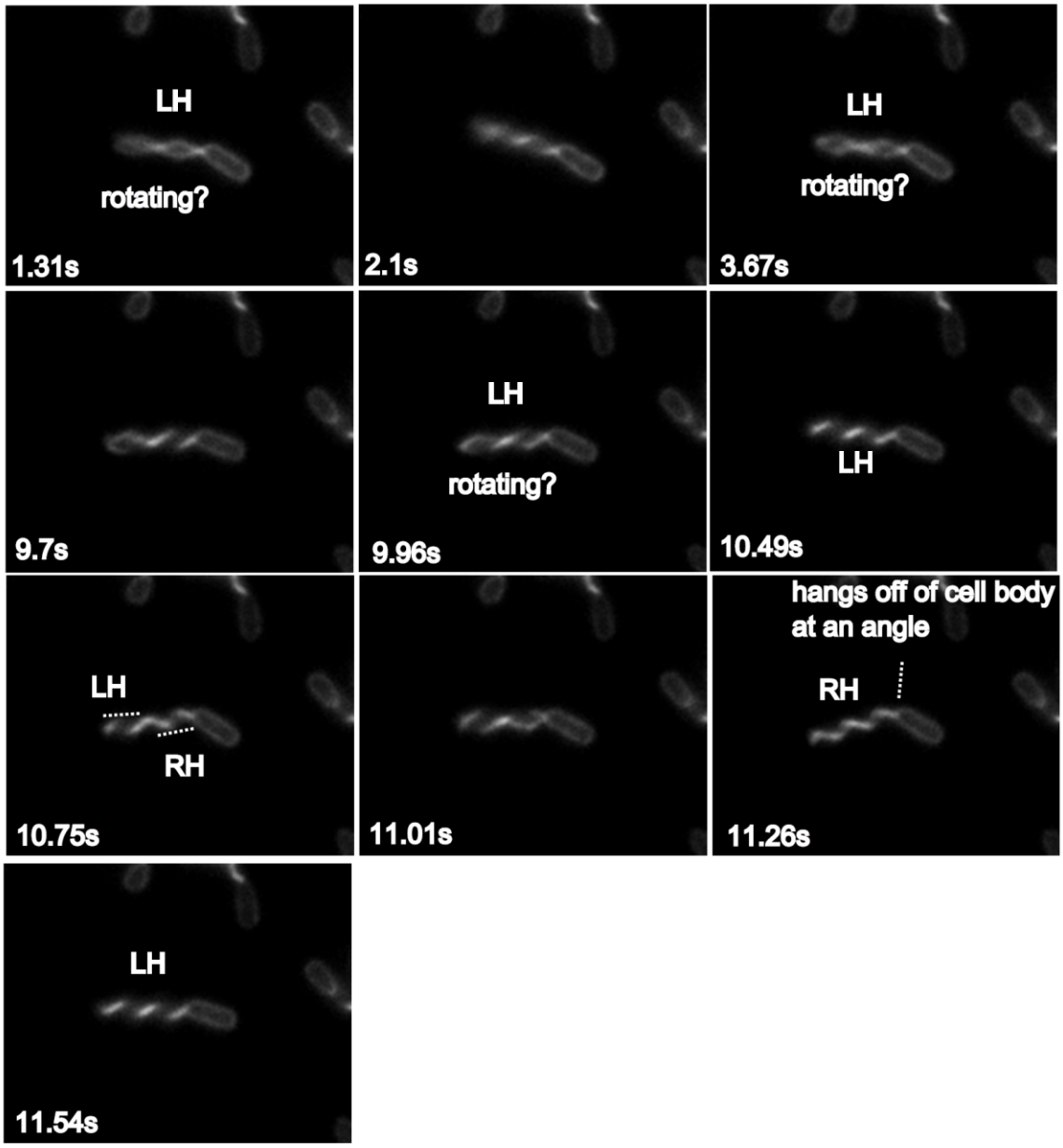

Figure 10. Flagellar polymorphic transformations observed in a single cell. LH and RH are abrieviations for left and right handed respectively.

Chapter 4: Bacterial Second Messenger Diversity is Generated by the Chemotaxis Machinery

A Specific *P. aeruginosa* Phosphodiesterase is Required to Generate Low Intracellular CDG After Cell Division.

The process of asymmetric distribution results in heterogeneity in cellular CDG levels during exponential phase cell growth. Single time point measurements of cellular CDG levels from exponentially growing wild type cells therefore gave rise to a bimodal distribution of cellular CDG levels in which 20% of cells consistently exhibited CDG concentrations less than 200 nM (Figure 11A and 11E). To identify enzymes important in this process, a bank of strains with transposon insertions in genes encoding DGCs and PDEs was screened for alterations in cellular CDG concentrations. The PDE encoded by PA5017 (Kulasakara et al., 2006) was required for the maintenance of CDG levels less than 200 nM. PA5017 encodes an 899 amino acid protein with six domains (Figure 12A) including a C-terminal EAL domain conferring PDE activity. Strains with mutations in PA5017 have reduced flagellar motility (Li et al., 2007; Figure 12B) and dispersion from biofilms (Roy et al., 2012).This gene is referred to as *pac* for Phosphodiesterase associated with the chemotaxis machinery, for reasons described below. Strains with a *pac* in frame deletion gave rise to a distribution of cellular CDG levels where at least 99% of cells harbored CDG levels more than 200 nM, indicating its importance in the maintenance of low CDG concentrations (Figure 11B and 11E). Complementing the *pac* deletion by providing *pac* in single copy at the attTn7 site under control of its native promoter was sufficient to restore low cellular CDG, whereas complementing with a mutant *pac* encoding an

enzymatically inactive protein (E675A) was not (Figure 11C, 11D, and 11E), demonstrating that the PDE activity of Pac was required for the maintenance of low cellular CDG after cell division.

Pac Exhibits Polar Localization in Cells with Low CDG.

Asymmetry in CDG levels could occur through spatial organization of either PDEs or DGCs. Therefore a strain was constructed with a single copy C-terminal translational fusion of Pac to mCherry under control of its native promoter at the chromosomal attTn7. This fusion was enzymatically active and functional, as it restored the population of cells with low CDG in strains with the *pac* deletion (Figure 12C). Pac-mCherry exhibited polar localization (Figure 12D). When CDG levels and Pac-mCherry localization were simultaneously monitored using time-lapse imaging, Pac was enriched at the pole of those incipient daughter cells that exhibited lower CDG following cell division (Figure 13A and 12E). To measure the association between Pac-mCherry localization and lower cellular CDG, single time point images were processed to bin cells into two groups as determined by CDG level. Cells with CDG less than 200 nM were found to exhibit a median value of 63% (SD of 23%) greater polar fluorescence intensity and a median value of 24% (SD of 4%) greater cellular fluorescence intensity (Figure 13B and 13C). This correlation between polar localization of Pac and low CDG levels indicates that the asymmetry in CDG levels between progeny occurs largely through the differential polar localization of Pac.

A Functional Flagellar Secretion Apparatus and Flagellar Polarity are Required for Pac-mCherry Polar Localization.

It was previously shown that a functional flagellum was required for the maintenance of low CDG, suggesting Pac localization may also require an intact flagellum. To test this hypothesis, Pac localization was measured in a strain lacking *fliF*. The *fliF* mutant lacked polar localization of Pac-mCherry indicating that a flagellar component or intact flagellum is required for Pac localization and maintenance of low CDG (Figure 14A and 14D).

We also measured the effect of deleting *flhF* on Pac -mCherry localization. The FlhF protein was previously tested for its effect on CDG and found to be dispensable for the maintenance of low CDG. In an *flhF* deletion, the flagellum is nonpolar and polar localization of Pac -mCherry is altered such that foci are often observed at random positions that do not correspond to the pole (Figure 14B, 14C and 14D). This result indicated that Pac requires *flhF* for its polar placement perhaps indirectly because the flagellar complex or an uncharacterized complex requires *flhF* for polar placement.

The Chemotaxis Machinery Protein CheA, Like the Flagellum, is Localized to a Pole, but is Delocalized in an *flhF* Mutant.

Only the flagellar apparatus has been characterized to require FlhF for its polar placement. However, the chemotaxis machinery is also localized to the pole of the cell (Guvener et al., 2006) and requires an intact flagellar basal body rod-hook structure for its expression (Dasgupta et al., 2003). Therefore it was plausible that Pac activity and/or localization could be directly dependent on the chemotaxis machinery rather than the flagellum. It was unknown but plausible that the chemotaxis machinery also requires FlhF for polar placement because of its involvement in motility. Therefore, a functional C-terminal fusion of the chemotaxis histidine kinase CheA to mTurquoise2 (mTq) was constructed (Figure 15A). Whereas 52% of wild type cells exhibited

polar localization of CheA-mTq, this dropped to 23% in Δ*flhF* mutant cells (Figure 16A) (Figure 16B). When CheA-mTq localization was monitored together with FliM-mKate2, foci were present at the same pole in 87% of cells (Figure 15B and 15C) indicating CheA-mTq is assembled at the flagellated pole. In summary, CheA-mTq exhibits localization to the same pole as the flagellum, a process that is dependent upon *flhF*.

The Chemotaxis Machinery Protein CheA is Required for Polar Localization of Pac and Maintenance of Low CDG.

The above data indicated that Pac polar localization could be directly dependent on a chemotaxis machinery protein. The *P. aeruginosa* chemotaxis cluster is similar to that of *E. coli,* and based on phenotypes of mutant strains, the function of individual components appears to be conserved between the two organisms (Ferrández et al., 2002; Schmidt et al., 2011). Therefore, a variety of strains with mutations in the chemotaxis cluster were assayed for an effect on Pac polar localization and low CDG after cell division. Strains with deletions in *cheR, cheY*, and *cheB* demonstrated no effect on Pac localization and cellular CDG levels. In contrast, a mutant in the histidine kinase *cheA* demonstrated a significant defect in Pac localization. This defect was complemented by expression of *cheA in trans* from a plasmid (Figure 17A and 17B). Additionally, CDG in the *cheA* deletion was significantly increased relative to wild type (Figure 17C and 17D). It was feasible that the cell not only requires CheA to generate low CDG in a single daughter cell but also integrates the activity of the chemotaxis system in the control of cellular CDG levels. *E. coli* CheA possesses a conserved phosphorylated histidine residue that is essential to its function, which is also conserved in *P. aeruginosa* CheA (Hess et al., 1988). Therefore a *P. aeruginosa* strain was constructed with a CheAHis49N allele located at the native

chromosomal position. Although swimming motility data indicated this residue is important for chemotaxis signal transduction (Figure 15D), it had very little effect on Pac-mCherry localization (Figure 17A) indicating signal transduction is not required for Pac localization. CDG levels were measured in this strain as well as in another strain that exhibits reduced CheA phosphorylation, a *cheR* deletion that abrogates methylation of MCPs and reduces downstream activity of CheA. Although polar localization of Pac was maintained in both strains, CDG levels increased relative to wild type (Figure 17D) as more than 90% of cells exhibited greater than 200 nM intracellular CDG levels. This suggested that full maintenance of low CDG requires phosphorylation of CheA, and that external information sensed by the chemotaxis machinery may be translated into Pac activity. Additionally, if Pac forms a complex with CheA, then the two proteins should exhibit colocalization. Therefore the distance between the centers of foci formed by CheA-mTQ and Pac-Yfp was measured in individual cells (Figure 16C). The median distance between focus centers in both wild type and Δ*flhF* backgrounds was less than 0.180 □m (Figure 16D), again supporting the conclusion that the two proteins associate or are part of a protein complex. In contrast is the larger median separation found between FliM-mKate2 and CheA-mTQ2 foci (Figure 15B and 15C) where there is no evidence of association between these individual components of different protein complexes. Finally, localization of FliM-mKate2 to the cell pole appeared to be similar (Figure 15E) between wild type and the *cheA* deletion indicating that although chemotaxis machinery assembly is dependent upon an assembled basal body hook and rod structure, flagellar assembly is not dependent upon a functional chemotaxis machinery. Therefore, low cellular CDG requires the chemotaxis machinery and not the flagellar apparatus to maintain CDG polarity, and *cheA* is required for Pac polar localization and is essential for the maintenance of CDG asymmetry after cell division. Pac likely binds directly to

CheA or another unknown closely associated protein. The name Pac has thus been derived from chemotaxis associated phosphodiesterase as the CheA protein is required for polar localization and activity of the phosphodiesterase.

Discussion

In this work a PDE, termed Pac, was identified as necessary for generating CDG asymmetry following cell division. Cells that exhibited lower CDG after cell division also exhibited greater cellular levels and increased polar localization of Pac. Therefore, heterogeneity in CDG levels is generated through Pac spatial localization. Pac alone does not contain the information to migrate to the relevant cell pole, as the chemotaxis protein CheA was also required for Pac partitioning and low CDG. Pac polar localization alone is not required for low CDG, as low CDG was still observed in the FlhF mutant, which delocalizes CheA from the pole. An interaction with CheA likely results in specific allosteric regulation of Pac, since low CDG is not observed in the CheA mutants and the CheA phosphoacceptor residue is required for maximum reduction in CDG levels. These observations indicate a model (Figure 18) for the generation of asymmetrical CDG concentrations and cellular diversity after cell division. Chemotaxis machinery protein CheA is localized to the flagellated cell pole and recruits Pac to this single daughter cell pole following cell division. Pac, upon binding to the Chemotaxis machinery through CheA, preferentially acts in this cell to generate a drop in the CDG concentration. Therefore the generation of CDG heterogeneity is a process that is dictated by unequal inheritance of an enzyme dependent on external signals and partitioning of the chemotaxis machinery. This provides an important molecular link between the chemotaxis machinery and CDG, and may be a general mechanism by which bacteria generate diversity after cell division.

Interestingly, polar localization of Pac and CheA require *flhF*. This encodes a signal recognition particle like protein required for polar localization of the flagellum in monotrichous bacteria such as *P. aeruginosa* (Murray et al., 2006). Though FlhF was known to promote localization of the flagellar apparatus, it was not known that the chemotaxis machinery itself required FlhF for polar localization. The ATPase ParC promotes polar localization of the chemotaxis machinery in the polarly flagellated bacterium *Vibrio cholera* (Ringgaard et al., 2011). In contrast, models for polar placement of the *E. coli* chemotaxis machinery, an organism with multiple peritrichous flagella, suggest it independently arrives at the pole through the action of stochastic self-assembly (Greenfield et al., 2009). These two findings indicate that the polar localization of the chemotaxis machinery is different in peritrichous bacteria, though it raises the interesting possibility that an unknown protein in peritrichous bacteria analogous to FlhF or ParC promotes polar localization of the chemotaxis machinery.

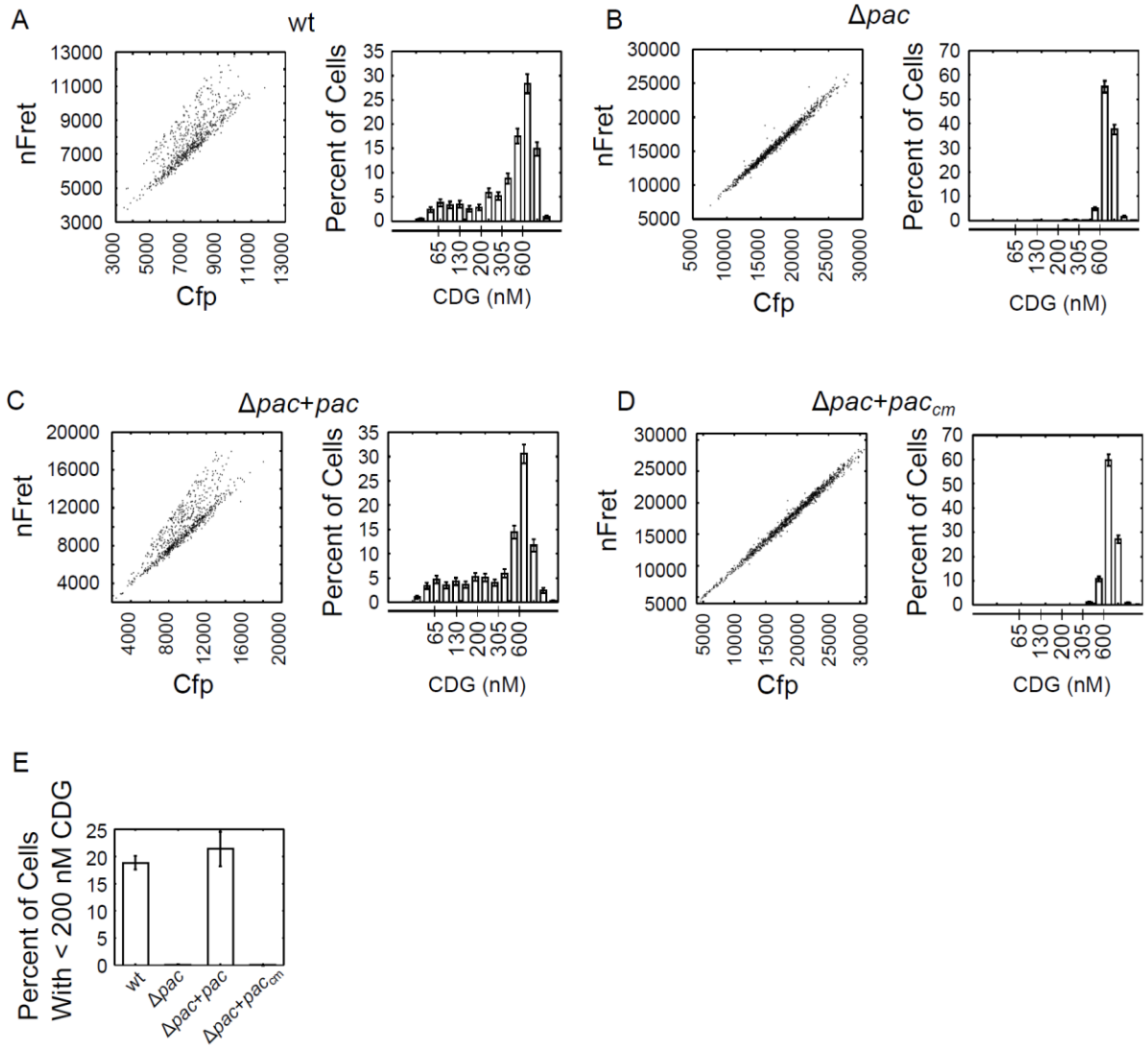

Figure 11. PA5017/Pac is required for wild type levels of CDG. A) Biosensor activity in individual wild type cells. The scatter plot on the left depicts mean nFret values versus Cfp values per cell. A histogram of cellular CDG levels is shown on the right where error bars depict the counting error. All subsequent panels represent graphical data in the same manner as in panel A. B) Biosensor activity in Δ*pac*. C) Biosensor activity in Δ*pac* complemented with *pac*. D) Biosensor activity in Δ*pac* complemented with a catalytic mutant of Δ*pac*. E) Quantification of the mean percentage of cells with less than 200 nM CDG from three biological replicates. Error bars depict the standard deviation.

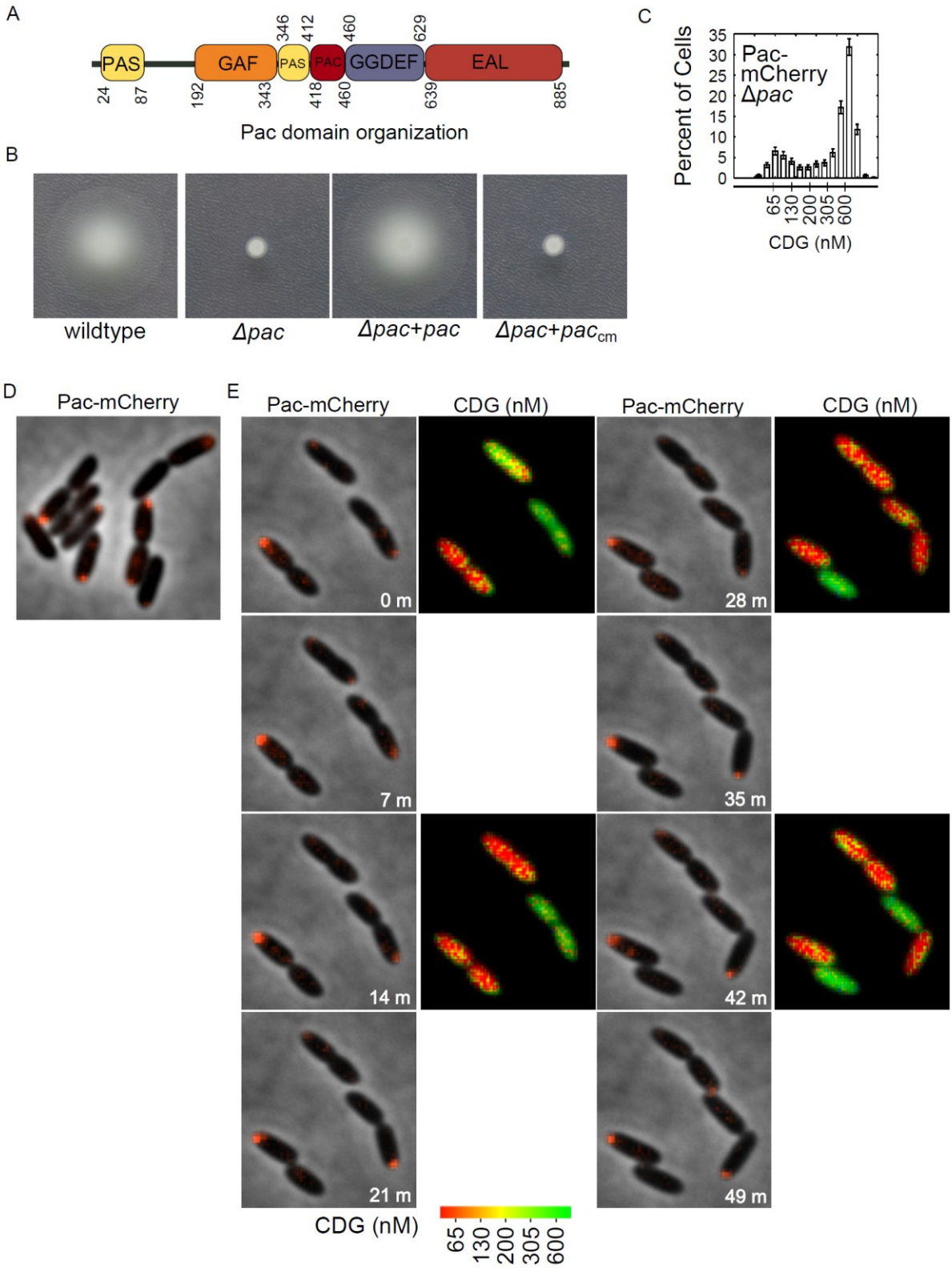

Figure 12. Features of PA5017/Pac. A) Pac domain organization. B) Swimming motility assay of a *pac* deletion. C) Biosensor activity in a *pac* deletion complemented with Pac-mCherry; 30.3% (SD of 5.9%) of cells exhibited less than 200 nM CDG. D) Pac-mCherry localization. An overlay of the fluorescence image (red) and phase image is shown. E) Pac-mCherry localization in combination with CDG levels over time.

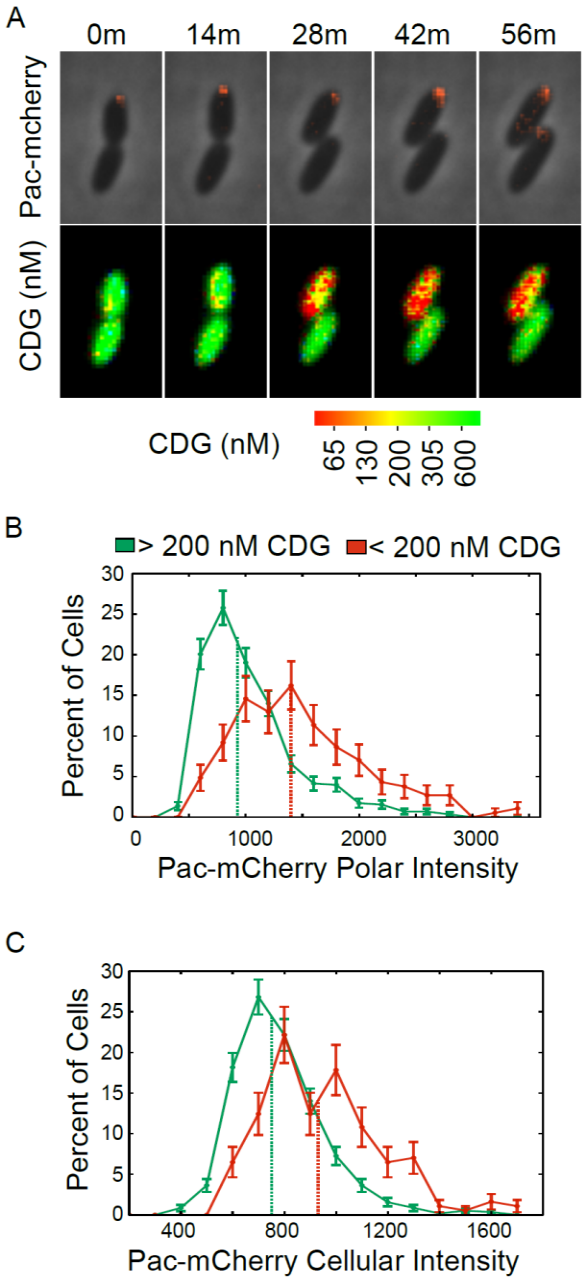

Figure 13. Polar localization of Pac-mCherry is associate with low cellular CDG after cell division. A) A time lapse image of biosensor activity and Pac-mCherry localization in a dividing cell. The top panel shows an overlay of the fluorescence channel (in red) and the phase contrast image. The bottom panel shows pseudocolored images depicting the CDG concentration, as indicated by the scale below. B) Distribution of the (brighter of the two) polar Pac-mCherry intensities of cells binned according to CDG. Dotted vertical lines mark the median value. Error bars depict the counting error. C) A histogram of mean Pac-mCherry cellular intensities when binned into two groups as in B). Other features from B) apply to C).

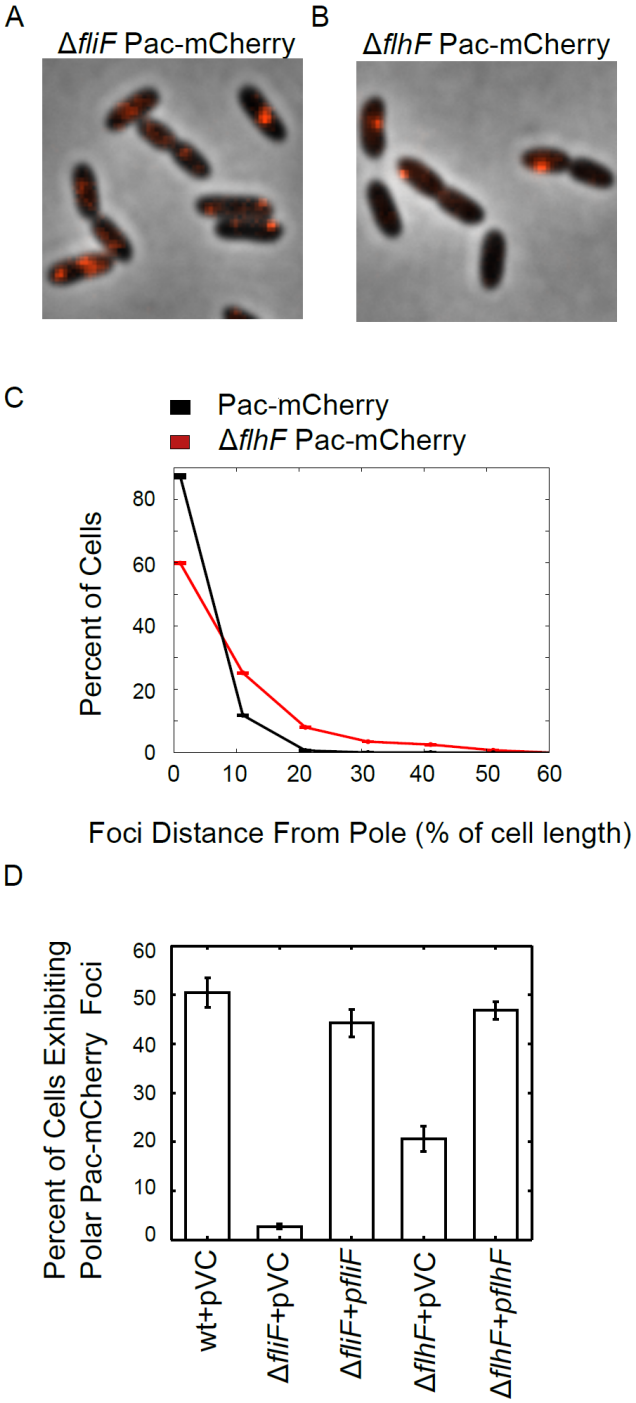

Figure 14. A funtional flagellar secretion apparatus and flagellar polarity are required for Pac-mCherry polar localization. A) Pac-mCherry localization in a Δ*fliF* mutant. B) Pac-mCherry localization in an Δ*flhF* mutant. C) Histograms of Pac-mCherry foci distances to the nearest pole in wild type and Δ*flhF* mutant backgrounds. D) A plot of the percent of cells exhibiting polar Pac-mCherry foci in different flagellar mutants.

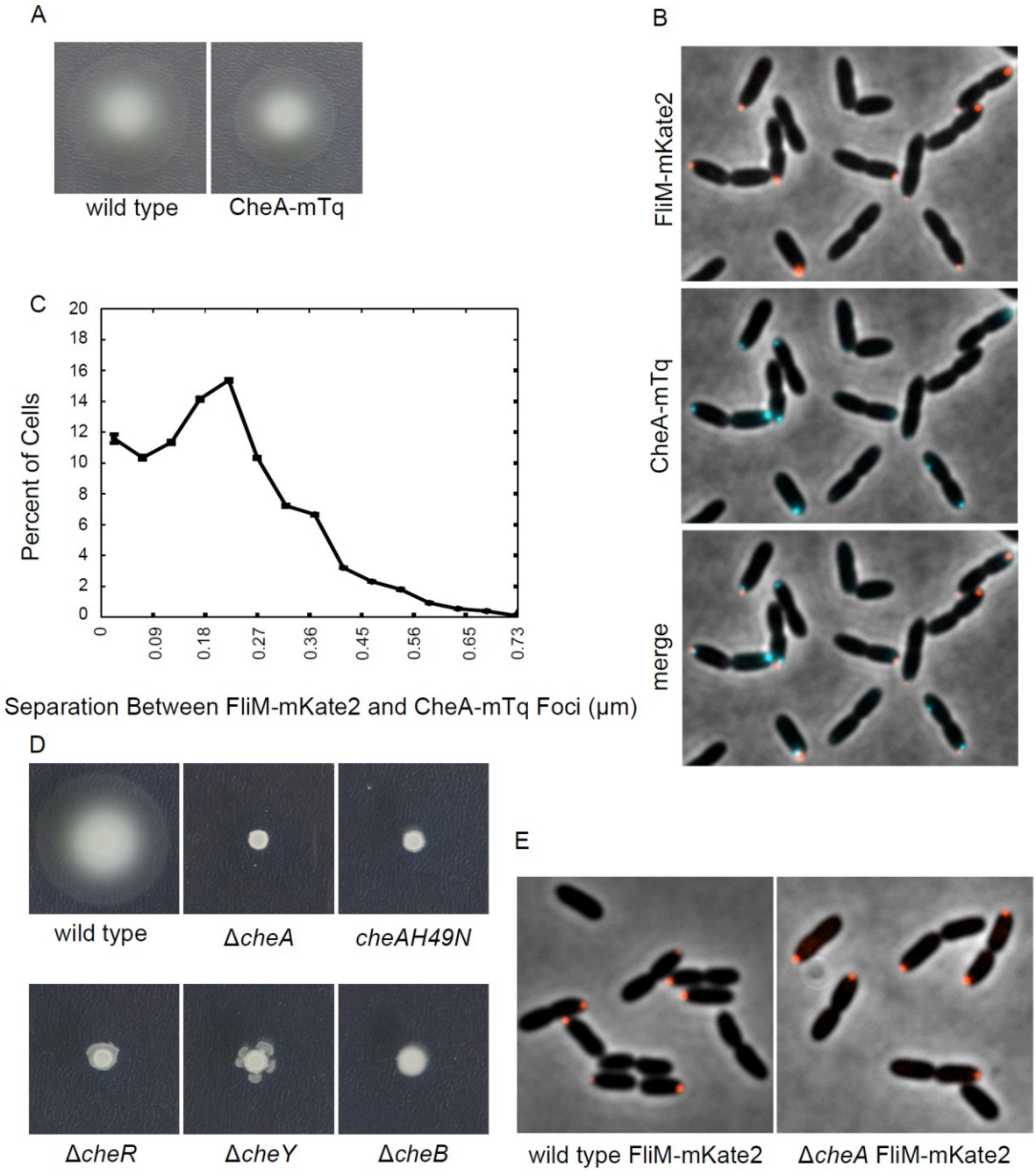

Figure 15. CheA-mTq is functional and localizes to the same pole as FliM-mKate2. A) Swimming motility of the CheA-mTq fusion strain as compared to wild type. B) CheA-mTq and FliM-mKate2 localization. C) A histogram of the minimum separation between CheA-mTq and FliM-mKate2 foci per cell. D) Swimming motility of chemotaxis mutants. CheA Histidine 49 is required for wild type motility. The other mutants show the expected motility attenuation. E) FliM-mKate2 localization in wild type and Δ*cheA* backgrounds; 39.7% (SD of 4.5%) of wild type cells exhibit polar localization and 40.7% (SD of 3.6%) of Δ*cheA* cells exhibit polar localization indicating it is not required for flagellar assembly.

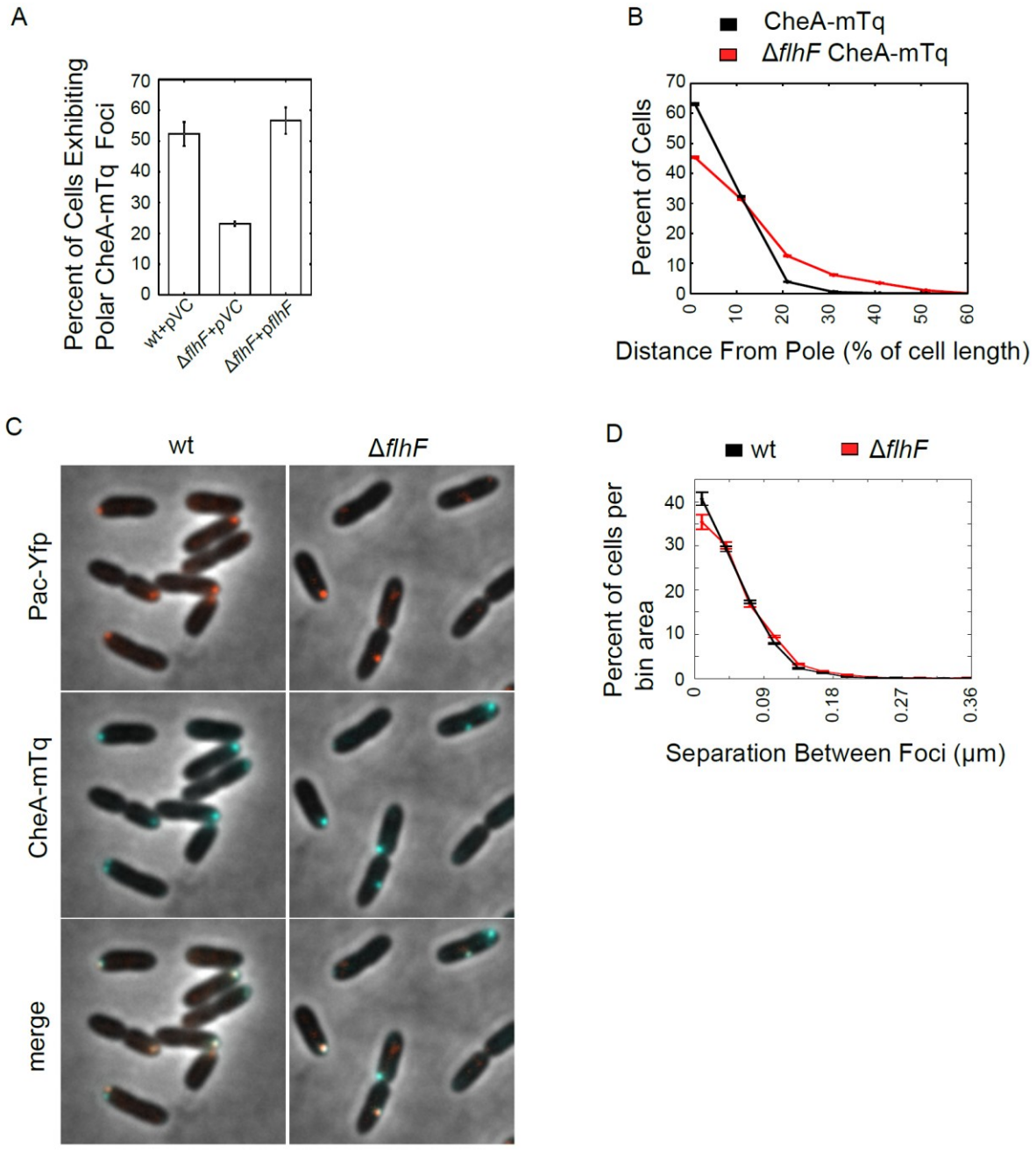

Figure 16. CheA is reliant on *flhF* for polar placement and CheA-mTq colocalizes with Pac-Yfp in wild type and Δ*flhF* backgrounds. A) Percent of cells exhibiting polar CheA-mTq foci in wild type and Δ*flhF* strain backgrounds. Strains contain empty vector (pVC) or a complementing plasmid. B) Histogram of the CheA-mTq foci distances from the closest cell pole in wild type and *flhF* deletion strains. Dotted vertical line marks the median values. C) CheA-mTq and Pac-Yfp localization in wild type and Δ*flhF* strains. CheA-mTq fluorescence is shown in blue and Pac-Yfp fluorescence is shown in red. D) Histogram of the closest distance between any two CheA-mTq and Pac-Yfp foci in wild type and Δ*flhF* strain backgrounds.

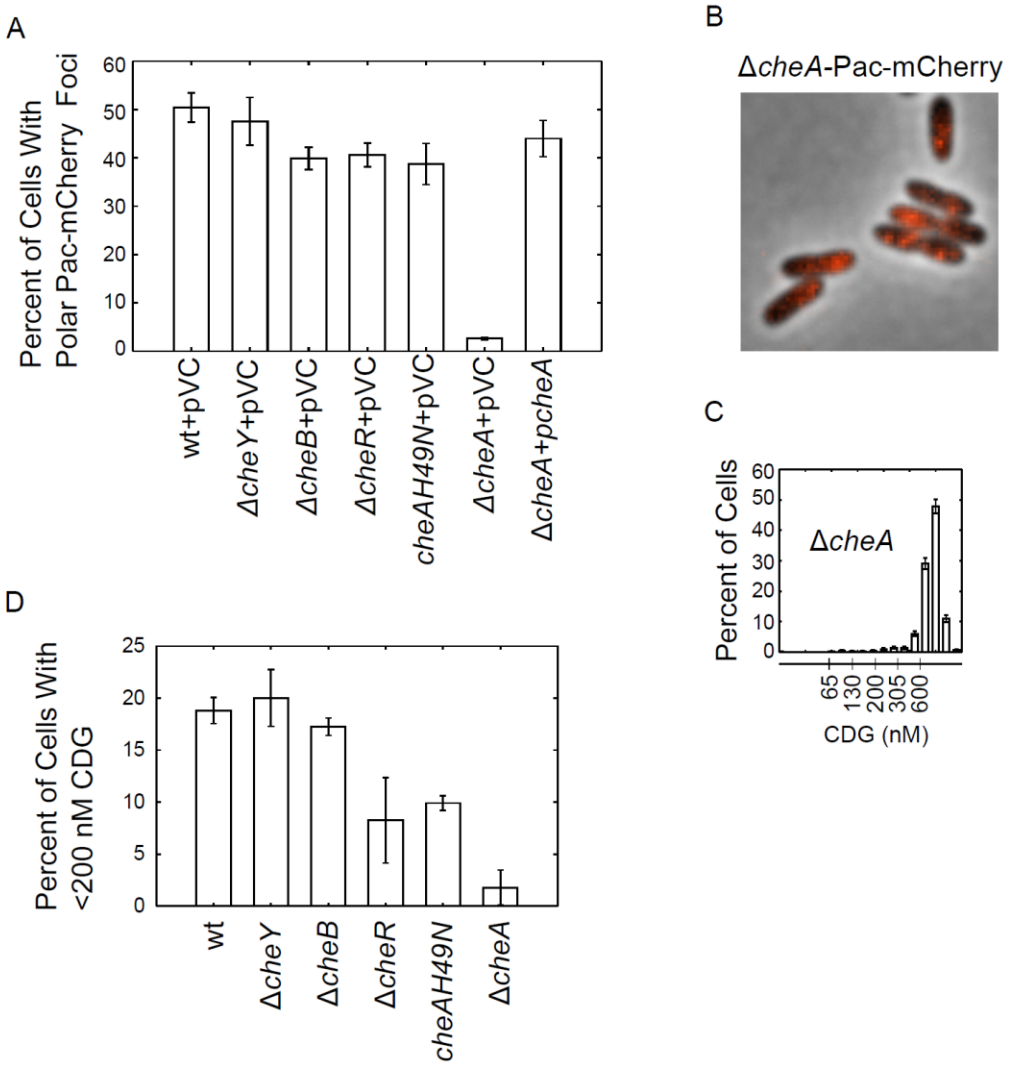

Figure 17. CheA is required for the maintenance of low CDG and polar localization of Pac-mCherry. A) Quantification of the percent of cells exhibiting polar localization of Pac-mCherry in different strain backgrounds. Strains contain empty vector (pVC) or a complementing plasmid. B) Pac-mCherry localization in a *cheA* deletion mutant. Shown is an overlay of the fluorescence image and phase contrast image. C) A histogram of cellular CDG levels in the *cheA* deletion. D) A graph of the mean percentage of cells with less than 200 nM CDG from three biological replicates. Error bars depict the standard deviation.

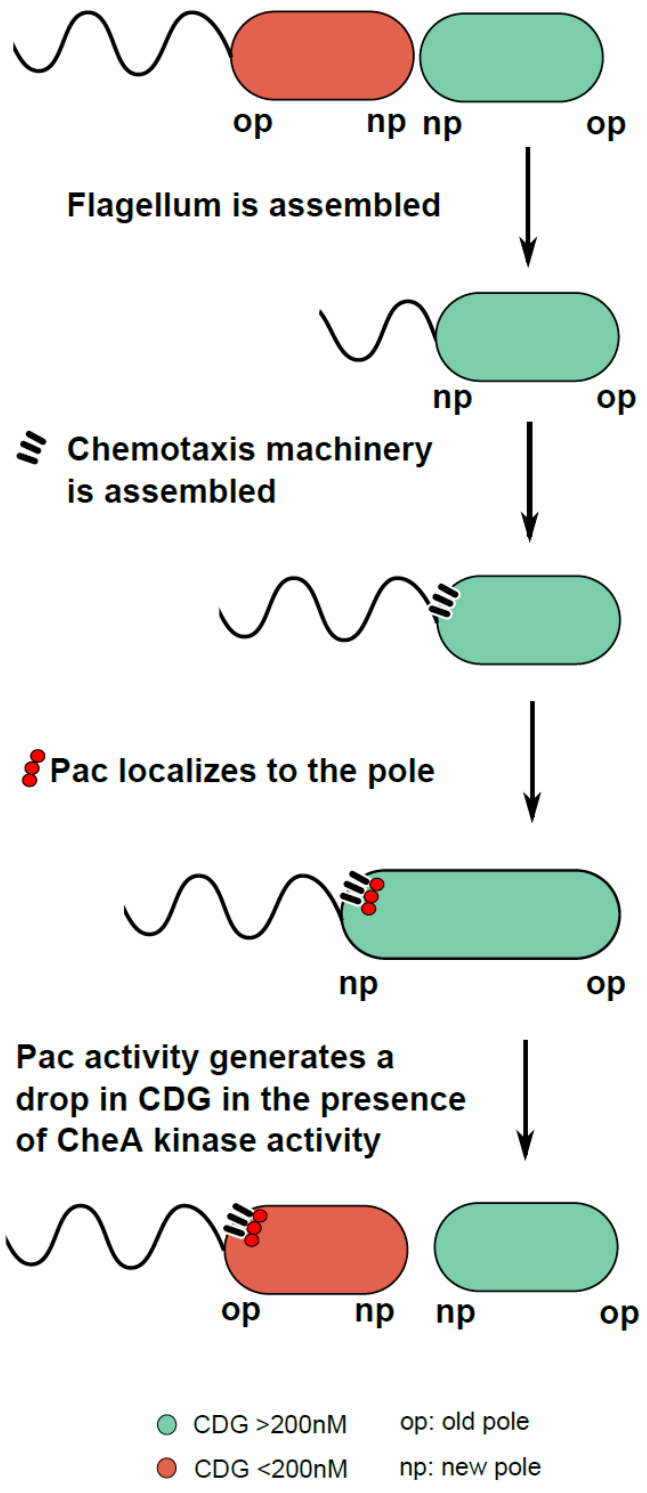

Figure 18. Model of how heterogeneity in CDG levels are generated in *P. aeruginosa*

Chapter 5: Conclusions and Perspectives

Conclusions

In this work, we utilized a novel biosensor to characterize intracellular CDG levels in bacterial cells. We determined that CDG is often distributed asymmetrically following cell division in *C. crescentus* and *P. aeruginosa* where the flagellated daughter cell in both species exhibits lower levels of CDG. In *C. crescentus*, it was known that dynamic localization of the DGC, PleD to the incipient stalked cell pole is required for the generation of asymmetry. In *P. aeruginosa*, this observation was unexpected and therefore uncharacterized. We subsequently determined that this asymmetry is dependent upon the PDE, PA5017/*pac*. This PDE localizes to the pole of the cell that exhibits a drop in CDG, and is dependent upon both the flagellum and chemotaxis protein, CheA, for its localization. Further dissection of this process indicated that Pac binds to the chemotaxis machinery protein CheA, or a protein associated with CheA. We subsequently determined that activity of the chemotaxis protein, CheA, is required for the maintenance of low CDG.

Biochemical Characterization of Pac.

It is likely that Pac binds CheA or another CheA binding protein. One alternative binding partner is a homologue of the ParC like ATPase required for chemotaxis machinery assembly in *Vibrio cholerae*. Other possible binding partners are methyl accepting chemotaxis proteins. Mutants in a transposon bank can be investigated for their effects on Pac localization. Further biochemical characterization can be performed to investigate the possibility that Pac binds CheA directly. Along these lines, we have attempted several times to purify Pac, however attempts to overexpress this protein in a heterologous system have resulted in very low yields of soluble

protein. Additional efforts will be made to either increase its expression or to scale up production. We have, however, successfully purified *P. aeruginosa* CheA. Once we have successfully purified Pac, we will determine whether the two proteins associate utilizing size exclusion chromatography and whether CheA activates Pac PDE activity.

Possible Biological Effects

Intracellular concentrations of CDG can lead to dampening of bacterial swimming motility through CDG binding to the flagellar brake YcgR. This has been characterized in *E. coli* and *Salmonella typhimurium* in which YcgR has an affinity for CDG of 180-190 nM (Christen et al., 2007). Above an intracellular CDG concentration of 180-190 nM, YcgR slows the motor rotation speed and biases the motor to rotate in a CCW direction. High CDG also inhibits *P. aeruginosa* swimming motility and biases CCW motor rotation (Merritt et al., 2007). *P. aeruginosa* possesses a homologue of YcgR which has two affinities for CDG of 88 nM and 732 nM (Pultz et al., 2012) and likely exhibits control over flagellar motility by the same mechanism. In contrast to the regulatory mechanism of YcgR, the chemotaxis system facilitates navigation along chemical gradients by controlling the frequency of directed runs and tumbling (or reversals, and random reorientation events in *P. aeruginosa*). This is accomplished by altering the frequency of CCW and CW motor rotation events. The observation that maintenance of low CDG requires the flagellar apparatus and chemotaxis machinery indicates an important function of heterogeneity of CDG in *P. aeruginosa* may be to impact chemotaxis. Using FliM-mKate2 as a marker for assembled flagellar apparatus, we determined that although flagellated cells were enriched for low CDG, they did not always exhibit low CDG levels, whereas non-flagellated cells generally experienced levels greater than 200nM. Because this diversity was restricted to

the chemotactic population, it is possible that the function of the observed variation in CDG levels is to generate a variety of chemotactic behaviors in response to a chemical gradient. This model somewhat contrasts with the view that CDG acts as a binary switch, initiating the transition between a motile and sessile lifestyle. There has been discussion on the presence of unexplained diversity in chemotactic populations of *E. coli* (Koshland, 1980) and it has been postulated that the diversification of responses could be advantageous when navigating chemical gradients in the environment (Sourjik and Wingreen, 2012). Therefore this work indicates a specific mechanism by which this could be accomplished.

To determine whether gradations in CDG truly generates a diversity of responses, single cell studies of chemotaxis should be carried out in the presence of artificially low and wild type levels of CDG. In addition, the effectors that result in swimming motility inhibition observed in the *pac* deletion need to be identified, where the YcgR homolog is a prime candidate. However, if the YcgR homolog proves to not mediate inhibition of motility, transposon mutagenesis studies can be performed to identify the effector proteins mediating this process.

The Extent of Heterogeneity

The complexity of intracellular *P. aeruginosa* CDG concentrations could be much greater than what we have observed utilizing the CDG biosensor with a range of detection of 65 nM to 600 nM. Approximately 50% percent of cells exhibited CDG levels which could only be measured as above 600 nM. As receptor affinities extend upwards of 12-20 μM and biological output is generated by cellular CDG concentration (Pultz et al., 2012; Shikuma et al., 2012), *P. aeruginosa* is likely to have significant differences in cellular concentrations above 600 nM. Therefore, in a population of cells this diversity of individuals can be maintained and rapidly

altered in a manner that should provide selective advantages in specific environmental conditions. This work indicates that these population differences are not simply stochastic but involve specific events associated with the cell cycle and the variation in cellular inheritance of specific organelles. In this regard it is interesting to speculate that the same will be the case for other organelles, such as flagella, which are inherited in an uneven fashion in peritrichously flagellated bacteria (Ping, 2010) or pili. Organelle based partitioning of cellular proteins could therefore be a broader mechanism by which bacteria generate cellular diversity after cell division within populations.

The Multiplicity of DGCs and PDEs

Efforts to elucidate the individual biological roles of CDG metabolizing enzymes commonly entail the measurement of swimming motility, exopolysaccharide formation, and/or biofilm formation in strains that overexpress or are deleted for relevant enzymes (Kulasakara et al., 2006). Some mutants give seemingly redundant phenotypes, leading to questions as to why the multiplicity of enzymes exists within individual bacterial genomes. This work, examining population wide heterogeneity indicates another plausible explanation for this diversity is that individual enzymes are required to generate specific levels of cellular CDG within a population of cells. Furthermore, additional diversity may be generated when these enzymes are regulated by binding to specific protein partners and specific cellular activation by external signals as we've observed with the reliance on CheA phosphorylation. Allosteric regulation dependent upon the presence of signal transduction cascades has already been shown to control activity of several enzymes including the *P. aeruginosa* DGC, WspR (Hickman et al., 2005). Additionally, it has already been shown for several enzymes that expression of specific enzymes varies

dependent upon growth phase (Weber et al., 2006). Therefore the number and diversity of CDG metabolizing enzymes may be utilized through expression levels, subcellular localization, specific cellular partitioning, and allosteric regulation to generate a range of distinct cellular CDG levels resulting in diverse individual cell behaviors.

What can be done in subsequent work to prove this hypothesis? Increasing the range of detection using additional biosensors with varying affinities will help to characterize the true extent of variation in cellular CDG levels and subsequently help to provide a greater context for the role of individual enzymes. Preliminary work has already been done using a biosensor with a lower affinity to determine that a significant population of (PA14) cells (> 20%) exhibit cellular CDG levels even above 3.2 μm. Secondly, the screen of transposon mutants was performed in the PA01 background. A significant portion of cells exhibited low CDG meaning that this screen was biased towards identifying PDEs. In PA14, cells predominantly exhibit levels of CDG greater than 200 nM. Therefore, a more sensitive screen for DGCs that generate CDG under these experimental conditions can be repeated in PA14. As we hypothesize these enzymes act in specific cell populations, we can then knock them out in combination to determine whether their effects are additive. As we hypothesize their mode of action is determined by partitioning to specific cell populations, we can make fusions to fluorescent proteins to determine whether they differentially localize to cell populations exhibiting specific levels of CDG.

In summary, this work contributes to our understanding of heterogeneity found in dividing bacterial populations. One mechanism of generating diversity within a population is to control the levels of a second messenger that has profound and diverse effects on cellular behavior. In addition if the system for partitioning and control of enzymatic activity integrates extracellular information to regulate the second messenger, a mechanism to generate significant

heterogeneity has been created. While it may be logical to assume that evolutionarily ancient single cell organisms like bacteria are homogeneous in composition, a growing body of work suggests they exhibit significant diversity similar to that of multicellular organisms (Rotem et al., 2010; Aldridge et al., 2012). Interestingly, they also share a mechanism for generating diversity; asymmetric cell division in multicellular organisms is a common developmental process by which daughter cells assume different fates as a result of unequal partitioning of cellular components (Rudel and Sommer, 2003; Morrison and Kimble, 2006). The diversity of individuals in a population undoubtedly is an evolutionary adaptive process that insures survival and promotion of the species in difficult environments and was likely adapted long before the evolution of multicellular organisms.

References

Aldridge, B., Fernandez-Suarez, M., Heller, D., Ambravaneswaran, V., Irimia, D., Toner, M., and Fortune, S. (2012). Asymmetry and aging of mycobacterial cells lead to variable growth and antibiotic susceptibility. Science (New York, N.Y.) *335*, 100-4.

Altschuler, S.J., and Wu, L.F. (2010). Cellular Heterogeneity: Do Differences Make a Difference? Cell *141*, 559-563.

Amikam, D., and Galperin, M. (2006). PilZ domain is part of the bacterial c-di-GMP binding protein. Bioinformatics (Oxford, England) *22*, 3-6.

An, S., Wu, J., and Zhang, L. (2010). Modulation of Pseudomonas aeruginosa biofilm dispersal by a cyclic-Di-GMP phosphodiesterase with a putative hypoxia-sensing domain. Applied And Environmental Microbiology *76*, 8160-73.

Arora, S., Ritchings, B., Almira, E., Lory, S., and Ramphal, R. (1996). Cloning and characterization of Pseudomonas aeruginosa fliF, necessary for flagellar assembly and bacterial adherence to mucin. Infection And Immunity *64*, 2130-6.

Arora, S., Ritchings, B., Almira, E., Lory, S., and Ramphal, R. (1997). A transcriptional activator, FleQ, regulates mucin adhesion and flagellar gene expression in Pseudomonas aeruginosa in a cascade manner. Journal Of Bacteriology *179*, 5574-81.

Baraquet, C., Murakami, K., Parsek, M., and Harwood, C. (2012). The FleQ protein from Pseudomonas aeruginosa functions as both a repressor and an activator to control gene expression from the pel operon promoter in response to c-di-GMP. Nucleic Acids Research *40*, 7207-18.

Barends, T., Hartmann, E., Griese, J., Beitlich, T., Kirienko, N., Ryjenkov, D., Reinstein, J., Shoeman, R., Gomelsky, M., and Schlichting, I. (2009). Structure and mechanism of a bacterial light-regulated cyclic nucleotide phosphodiesterase. Nature *459*, 1015-8.

Beatson, S., Minamino, T., and Pallen, M. (2006). Variation in bacterial flagellins: from sequence to structure. Trends In Microbiology *14*, 151-5.

Benach, J., Swaminathan, S., Tamayo, R., Handelman, S., Folta-Stogniew, E., Ramos, J., Forouhar, F., Neely, H., Seetharaman, J., Camilli, A., et al. (2007). The structural basis of cyclic diguanylate signal transduction by PilZ domains. The EMBO Journal *26*, 5153-66.

Bermejo, C., Haerizadeh, F., Takanaga, H., Chermak, D., and Frommer, W. (2011). Optical sensors for measuring dynamic changes of cytosolic metabolite levels in yeast. Nature Protocols *6*, 1806-17.

Bharati, B., Sharma, I., Kasetty, S., Kumar, M., Mukherjee, R., and Chatterji, D. (2012). A full-length bifunctional protein involved in c-di-GMP turnover is required for long-term survival under nutrient starvation in Mycobacterium smegmatis. Microbiology (Reading, England) *158*, 1415-27.

Boehm, A., Kaiser, M., Li, H., Spangler, C., Kasper, C.A., Ackermann, M., Kaever, V., Sourjik, V., Roth, V., and Jenal, U. (2010). Second Messenger-Mediated Adjustment of Bacterial Swimming Velocity. Cell *141*, 1-10.

Boles, B., and McCarter, L. (2002). Vibrio parahaemolyticus scrABC, a novel operon affecting swarming and capsular polysaccharide regulation. Journal Of Bacteriology *184*, 5946-54.

Briegel, A., Li, X., Bilwes, A., Hughes, K., Jensen, G., and Crane, B. (2012). Bacterial chemoreceptor arrays are hexagonally packed trimers of receptor dimers networked by rings of kinase and coupling proteins. Proceedings Of The National Academy Of Sciences Of The United States Of America *109*, 3766-71.

Byrd, M., Sadovskaya, I., Vinogradov, E., Lu, H., Sprinkle, A., Richardson, S., Ma, L., Ralston, B., Parsek, M., Anderson, E., et al. (2009). Genetic and biochemical analyses of the Pseudomonas aeruginosa Psl exopolysaccharide reveal overlapping roles for polysaccharide synthesis enzymes in Psl and LPS production. Molecular Microbiology *73*, 622-38.

Calladine, C., Luisi, B., and Pratap, J. (2013). A “mechanistic” explanation of the multiple helical forms adopted by bacterial flagellar filaments. Journal Of Molecular Biology *425*, 914-28.

Chan, C., Paul, R., Samoray, D., Amiot, N., Giese, B., Jenal, U., and Schirmer, T. (2004). Structural basis of activity and allosteric control of diguanylate cyclase. Proceedings Of The National Academy Of Sciences Of The United States Of America *101*, 17084-9.

Chen, M.W., Kotaka, M., Vonrhein, C., Bricogne, G., Rao, F., Chuah, M.L.C., Svergun, D., Schneider, G., Liang, Z.-., and Lescar, J. (2012). Structural Insights into the Regulatory Mechanism of the Response Regulator RocR from Pseudomonas aeruginosa in Cyclic Di-GMP Signaling. Journal Of Bacteriology *194*, 4837-4846.

Chen, S., Beeby, M., Murphy, G.E., Leadbetter, J.R., Hendrixson, D.R., Briegel, A., Li, Z., Shi, J., Tocheva, E.I., M&uuml, A., et al. (2011). Structural diversity of bacterial flagellar motors. The EMBO Journal *30*, 2972-2981.

Chin, K., Lee, Y., Tu, Z., Chen, C., Tseng, Y., Yang, J., Ryan, R., McCarthy, Y., Dow, J., Wang, A., et al. (2010). The cAMP receptor-like protein CLP is a novel c-di-GMP receptor linking cell-cell signaling to virulence gene expression in Xanthomonas campestris. Journal Of Molecular Biology *396*, 646-62.

Christen, M., Christen, B., Allan, M.G., Folcher, M., Jenö, P., Grzesiek, S., Jenal, U., Christen, M., Christen, B., Allan, M.G., et al. (2007). DgrA is a member of a new family of cyclic diguanosine monophosphate receptors and controls flagellar motor function in Caulobacter crescentus. Proceedings Of The National Academy Of Sciences *104*, 1-7.

Christen, M., Christen, B., Folcher, M., Schauerte, A., and Jenal, U. (2005). Identification and characterization of a cyclic di-GMP-specific phosphodiesterase and its allosteric control by GTP. The Journal Of Biological Chemistry *280*, 30829-37.

Christen, M., Kulasekara, H.D., Christen, B., Kulasekara, B.R., Hoffman, L.R., Miller, S.I., Christen, M., Kulasekara, H.D., Christen, B., Kulasekara, B.R., et al. (2010). Asymmetrical Distribution of the Second Messenger c-di-GMP upon Bacterial Cell Division. Science *328*, 1-4.

Colvin, K., Gordon, V., Murakami, K., Borlee, B., Wozniak, D., Wong, G., and Parsek, M. (2011). The pel polysaccharide can serve a structural and protective role in the biofilm matrix of Pseudomonas aeruginosa. Plos Pathogens *7*, e1001264.

Conrad, J. (2012). Physics of bacterial near-surface motility using flagella and type IV pili: implications for biofilm formation. Research In Microbiology *163*, 619-29.

Conti, M., and Beavo, J. (2007). Biochemistry and physiology of cyclic nucleotide phosphodiesterases: essential components in cyclic nucleotide signaling. Annual Review Of Biochemistry *76*, 481-511.

D'Argenio, D., Calfee, M., Rainey, P., and Pesci, E. (2002). Autolysis and autoaggregation in Pseudomonas aeruginosa colony morphology mutants. Journal Of Bacteriology *184*, 6481-9.

Dasgupta, N., and Ramphal, R. (2001). Interaction of the Antiactivator FleN with the Transcriptional Activator FleQ Regulates Flagellar Number in Pseudomonas aeruginosa. Journal Of Bacteriology *183*, 6636-6644.

Dasgupta, N., Wolfgang, M.C., Goodman, A.L., Arora, S.K., Jyot, J., Lory, S., and Ramphal, R. (2003). A four-tiered transcriptional regulatory circuit controls flagellar biogenesis in Pseudomonas aeruginosa. Molecular Microbiology *50*, 809-824.

Davare, M., Avdonin, V., Hall, D., Peden, E., Burette, A., Weinberg, R., Horne, M., Hoshi, T., and Hell, J. (2001). A beta2 adrenergic receptor signaling complex assembled with the Ca2+ channel Cav1.2. Science (New York, N.Y.) *293*, 98-101.

Dhar, N., and McKinney, J. (2007). Microbial phenotypic heterogeneity and antibiotic tolerance. Current Opinion In Microbiology *10*, 30-8.

Drenkard, E., and Ausubel, F. (2002). Pseudomonas biofilm formation and antibiotic resistance are linked to phenotypic variation. Nature *416*, 740-3.

Duerig, A., Abel, S., Folcher, M., Nicollier, M., Schwede, T., Amiot, N., Giese, B., and Jenal, U. (2009). Second messenger-mediated spatiotemporal control of protein degradation regulates bacterial cell cycle progression. Genes &Amp; Development *23*, 1-13.

Dworkin, J. (2009). Cellular polarity in prokaryotic organisms. Cold Spring Harbor Perspectives In Biology *1*, a003368.

Elowitz, M., Levine, A., Siggia, E., and Swain, P. (2002). Stochastic gene expression in a single cell. Science (New York, N.Y.) *297*, 1183-6.

Fang, X., and Gomelsky, M. (2010). A post-translational, c-di-GMP-dependent mechanism regulating flagellar motility. Molecular Microbiology *76*, 1-11.

Ferreira, R., Antunes, L., Greenberg, E., and McCarter, L. (2008). Vibrio parahaemolyticus ScrC modulates cyclic dimeric GMP regulation of gene expression relevant to growth on surfaces. Journal Of Bacteriology *190*, 851-60.

Ferrández, A., Hawkins, A.C., Summerfield, D.T., and Harwood, C.S. (2002). Cluster II che genes from Pseudomonas aeruginosa are required for an optimal chemotactic response. Journal Of Bacteriology *184*, 1-11.

Friedman, L., and Kolter, R. (2004a). Genes involved in matrix formation in Pseudomonas aeruginosa PA14 biofilms. Molecular Microbiology *51*, 675-90.

Friedman, L., and Kolter, R. (2004b). Two genetic loci produce distinct carbohydrate-rich structural components of the Pseudomonas aeruginosa biofilm matrix. Journal Of Bacteriology *186*, 4457-65.

Fürste, J., Pansegrau, W., Frank, R., Blöcker, H., Scholz, P., Bagdasarian, M., and Lanka, E. (1986). Molecular cloning of the plasmid RP4 primase region in a multi-host-range tacP expression vector. Gene *48*, 119-31.

Galkin, V., Yu, X., Bielnicki, J., Heuser, J., Ewing, C., Guerry, P., and Egelman, E. (2008). Divergence of quaternary structures among bacterial flagellar filaments. Science (New York, N.Y.) *320*, 382-5.

Galperin, M. (2001). Conserved "hypothetical" proteins: new hints and new puzzles. Comparative And Functional Genomics *2*, 14-8.

Galperin, M., Nikolskaya, A., and Koonin, E. (2001). Novel domains of the prokaryotic two-component signal transduction systems. FEMS Microbiology Letters *203*, 11-21.

Gibson, R., Burns, J., and Ramsey, B. (2003). Pathophysiology and management of pulmonary infections in cystic fibrosis. American Journal Of Respiratory And Critical Care Medicine *168*, 918-51.

Greenfield, D., McEvoy, A.L., Shroff, H., Crooks, G.E., Wingreen, N.S., Betzig, E., Liphardt, J., Group, B.G., Division, P.B., Institute, H.H., et al. (2009). Self-Organization of the Escherichia coli Chemotaxis Network Imaged with Super-Resolution Light Microscopy. Plos Biology *7*, e1000137.

Guvener, Z.T., Tifrea, D.F., and Harwood, C.S. (2006). Two different Pseudomonas aeruginosa chemosensory signal transduction complexes localize to cell poles and form and remould in stationary phase. Molecular Microbiology *61*, 1-13.

Guzman, L., Belin, D., Carson, M., and Beckwith, J. (1995). Tight regulation, modulation, and high-level expression by vectors containing the arabinose PBAD promoter. Journal Of Bacteriology *177*, 4121-30.

Guzzo, C., Salinas, R., Andrade, M., and Farah, C. (2009). PILZ protein structure and interactions with PILB and the FIMX EAL domain: implications for control of type IV pilus biogenesis. Journal Of Molecular Biology *393*, 848-66.

Güvener, Z., and Harwood, C. (2007). Subcellular location characteristics of the Pseudomonas aeruginosa GGDEF protein, WspR, indicate that it produces cyclic-di-GMP in response to growth on surfaces. Molecular Microbiology *66*, 1459-73.

Heikaus, C., Pandit, J., and Klevit, R. (2009). Cyclic nucleotide binding GAF domains from phosphodiesterases: structural and mechanistic insights. Structure (London, England : 1993) *17*, 1551-7.

Held, K., Ramage, E., Jacobs, M., Gallagher, L., and Manoil, C. (2012). Sequence-verified two-allele transposon mutant library for Pseudomonas aeruginosa PAO1. Journal Of Bacteriology *194*, 6387-9.

Hengge, R. (2009). Principles of c-di-GMP signalling in bacteria. Nature Reviews. Microbiology *7*, 263-73.

Henry, J., and Crosson, S. (2011). Ligand-binding PAS domains in a genomic, cellular, and structural context. Annual Review Of Microbiology *65*, 261-86.

Hess, J., Bourret, R., and Simon, M. (1988). Histidine phosphorylation and phosphoryl group transfer in bacterial chemotaxis. Nature *336*, 139-43.

Hickman, J.W., Tifrea, D.F., Harwood, C.S., Hickman, J.W., Hickman, J.W., Tifrea, D.F., and Harwood, C.S. (2005). A chemosensory system that regulates biofilm formation through modulation of cyclic diguanylate levels. Proceedings Of The National Academy Of Sciences *102*, 1-6.

Hickman, J., and Harwood, C. (2008). Identification of FleQ from Pseudomonas aeruginosa as a c-di-GMP-responsive transcription factor. Molecular Microbiology *69*, 376-89.

Hoang, T.T., Karkhoff-Schweizer, R.R., Kutchma, A.J., and Schweizer, H.P. (1998). A broad-host-range Flp-FRT recombination system for site-specific excision of chromosomally-located DNA sequences: application for isolation of unmarked Pseudomonas aeruginosa mutants. Gene *212*, 1-10.

Hoffman, L.R., D'Argenio, D.A., MacCoss, M.J., Zhang, Z., Jones, R.A., and Miller, S.I. (2005). Aminoglycoside antibiotics induce bacterial biofilm formation. Nature *436*, 1171-1175.

Huang, B., Whitchurch, C., and Mattick, J. (2003). FimX, a multidomain protein connecting environmental signals to twitching motility in Pseudomonas aeruginosa. Journal Of Bacteriology *185*, 7068-76.

Huitema, E., Pritchard, S., Matteson, D., Radhakrishnan, S., and Viollier, P. (2006). Bacterial birth scar proteins mark future flagellum assembly site. Cell *124*, 1025-37.

Häussler, S., Tümmler, B., Weissbrodt, H., Rohde, M., and Steinmetz, I. (1999). Small-colony variants of Pseudomonas aeruginosa in cystic fibrosis. Clinical Infectious Diseases : An Official Publication Of The Infectious Diseases Society Of America *29*, 621-5.

Häussler, S., Ziegler, I., Löttel, A., Götz, F., Rohde, M., Wehmhöhner, D., Saravanamuthu, S., Tümmler, B., and Steinmetz, I. (2003). Highly adherent small-colony variants of Pseudomonas aeruginosa in cystic fibrosis lung infection. Journal Of Medical Microbiology *52*, 295-301.

Irie, Y., Borlee, B., O'Connor, J., Hill, P., Harwood, C., Wozniak, D., and Parsek, M. (2012). Self-produced exopolysaccharide is a signal that stimulates biofilm formation in Pseudomonas aeruginosa. Proceedings Of The National Academy Of Sciences Of The United States Of America *109*, 20632-6.

Jacobs, M., Alwood, A., Thaipisuttikul, I., Spencer, D., Haugen, E., Ernst, S., Will, O., Kaul, R., Raymond, C., Levy, R., et al. (2003). Comprehensive transposon mutant library of Pseudomonas aeruginosa. Proceedings Of The National Academy Of Sciences Of The United States Of America *100*, 14339-44.

Jenal, U. (2004). Cyclic di-guanosine-monophosphate comes of age: a novel secondary messenger involved in modulating cell surface structures in bacteria? Current Opinion In Microbiology *7*, 185-91.

Johnson, J., Murphy, C., Sippy, J., Johnson, T., and Clegg, S. (2011). Type 3 fimbriae and biofilm formation are regulated by the transcriptional regulators MrkHI in Klebsiella pneumoniae. Journal Of Bacteriology *193*, 3453-60.

Jung, K., Fried, L., Behr, S., and Heermann, R. (2012). Histidine kinases and response regulators in networks. Current Opinion In Microbiology *15*, 118-24.

Khlebnikov, A., Datsenko, K., Skaug, T., Wanner, B., and Keasling, J. (2001). Homogeneous expression of the P(BAD) promoter in Escherichia coli by constitutive expression of the low-affinity high-capacity AraE transporter. Microbiology (Reading, England) *147*, 3241-7.

Kim, M., Bird, J., Parys, A., Breuer, K., and Powers, T. (2003). A macroscopic scale model of bacterial flagellar bundling. Proceedings Of The National Academy Of Sciences Of The United States Of America *100*, 15481-5.

Kirisits, M., Prost, L., Starkey, M., and Parsek, M. (2005). Characterization of colony morphology variants isolated from Pseudomonas aeruginosa biofilms. Applied And Environmental Microbiology *71*, 4809-21.

Klebensberger, J., Birkenmaier, A., Geffers, R., Kjelleberg, S., and Philipp, B. (2009). SiaA and SiaD are essential for inducing autoaggregation as a specific response to detergent stress in Pseudomonas aeruginosa. Environmental Microbiology *11*, 3073-86.

Ko, M., and Park, C. (2000). Two novel flagellar components and H-NS are involved in the motor function of Escherichia coli. Journal Of Molecular Biology *303*, 371-82.

Koshland, D. (1980). Bacterial chemotaxis in relation to neurobiology. Annual Review Of Neuroscience *3*, 43-75.

Krasteva, P., Fong, J., Shikuma, N., Beyhan, S., Navarro, M., Yildiz, F., and Sondermann, H. (2010). Vibrio cholerae VpsT regulates matrix production and motility by directly sensing cyclic di-GMP. Science (New York, N.Y.) *327*, 866-8.

Kuchma, S., Brothers, K., Merritt, J., Liberati, N., Ausubel, F., and O'Toole, G. (2007). BifA, a cyclic-Di-GMP phosphodiesterase, inversely regulates biofilm formation and swarming motility by Pseudomonas aeruginosa PA14. Journal Of Bacteriology *189*, 8165-78.

Kulasakara, H., Lee, V., Brencic, A., Liberati, N., Urbach, J., Miyata, S., Lee, D.G., Neely, A.N., Hyodo, M., Hayakawa, Y., et al. (2006). Analysis of Pseudomonas aeruginosa diguanylate cyclases and phosphodiesterases reveals a role for bis-(3“-5”)-cyclic-GMP in virulence. Proceedings Of The National Academy Of Sciences Of The United States Of America *103*, 2839-44.

Kulasekara, H., Ventre, I., Kulasekara, B., Lazdunski, A., Filloux, A., and Lory, S. (2005). A novel two-component system controls the expression of Pseudomonas aeruginosa fimbrial cup genes. Molecular Microbiology *55*, 368-80.

Kuo, J., and Greengard, P. (1969). Cyclic nucleotide-dependent protein kinases. IV. Widespread occurrence of adenosine -”,5”-monophosphate-dependent protein kinase in various tissues and phyla of the animal kingdom. Proceedings Of The National Academy Of Sciences Of The United States Of America *64*, 1349-55.

LeRoux, M., de Leon, J.A., Kuwada, N.J., Russell, A.B., Pinto-Santini, D., Hood, R.D., Agnello, D.M., Robertson, S.M., Wiggins, P.A., Mougous, J.D., et al. (2012). Quantitative single-cell characterization of bacterial interactions reveals type VI secretion is a double-edged sword. Proceedings Of The National Academy Of Sciences *109*, 1-6.

Lee, V., Matewish, J., Kessler, J., Hyodo, M., Hayakawa, Y., and Lory, S. (2007). A cyclic-di-GMP receptor required for bacterial exopolysaccharide production. Molecular Microbiology *65*, 1474-84.

Li, H., and Sourjik, V. (2011). Assembly and stability of flagellar motor in Escherichia coli. Molecular Microbiology *80*, 886-899.

Li, M., and Hazelbauer, G. (2011). Core unit of chemotaxis signaling complexes. Proceedings Of The National Academy Of Sciences Of The United States Of America *108*, 9390-5.

Li, Y., Xia, H., Bai, F., Xu, H., Yang, L., Yao, H., Zhang, L., Zhang, X., Bai, Y., Saris, P.E., et al. (2007). Identification of a new gene PA5017 involved in flagella-mediated motility, chemotaxis and biofilm formation in. FEMS Microbiology Letters *272*, 1-8.

Lister, P., Wolter, D., and Hanson, N. (2009). Antibacterial-resistant Pseudomonas aeruginosa: clinical impact and complex regulation of chromosomally encoded resistance mechanisms. Clinical Microbiology Reviews *22*, 582-610.

Macnab, R., and Ornston, M. (1977). Normal-to-curly flagellar transitions and their role in bacterial tumbling. Stabilization of an alternative quaternary structure by mechanical force. Journal Of Molecular Biology *112*, 1-30.

Malone, J., Jaeger, T., Manfredi, P., Dötsch, A., Blanka, A., Bos, R., Cornelis, G., Häussler, S., and Jenal, U. (2012). The YfiBNR signal transduction mechanism reveals novel targets for the

evolution of persistent Pseudomonas aeruginosa in cystic fibrosis airways. Plos Pathogens *8*, e1002760.

Malone, J., Jaeger, T., Spangler, C., Ritz, D., Spang, A., Arrieumerlou, C., Kaever, V., Landmann, R., and Jenal, U. (2010). YfiBNR mediates cyclic di-GMP dependent small colony variant formation and persistence in Pseudomonas aeruginosa. Plos Pathogens *6*, e1000804.

Massie, J., Reynolds, E., Koestler, B., Cong, J., Agostoni, M., and Waters, C. (2012). Quantification of high-specificity cyclic diguanylate signaling. Proceedings Of The National Academy Of Sciences Of The United States Of America *109*, 12746-51.

Mattick, J. (2002). Type IV pili and twitching motility. Annual Review Of Microbiology *56*, 289-314.

Meissner, A., Wild, V., Simm, R., Rohde, M., Erck, C., Bredenbruch, F., Morr, M., Römling, U., and Häussler, S. (2007). Pseudomonas aeruginosa cupA-encoded fimbriae expression is regulated by a GGDEF and EAL domain-dependent modulation of the intracellular level of cyclic diguanylate. Environmental Microbiology *9*, 2475-85.

Merighi, M., Lee, V., Hyodo, M., Hayakawa, Y., and Lory, S. (2007). The second messenger bis-(3“-5”)-cyclic-GMP and its PilZ domain-containing receptor Alg44 are required for alginate biosynthesis in Pseudomonas aeruginosa. Molecular Microbiology *65*, 876-95.

Merritt, J., Brothers, K., Kuchma, S., and O'Toole, G. (2007). SadC reciprocally influences biofilm formation and swarming motility via modulation of exopolysaccharide production and flagellar function. Journal Of Bacteriology *189*, 8154-64.

Merritt, J., Ha, D., Cowles, K., Lu, W., Morales, D., Rabinowitz, J., Gitai, Z., and O'Toole, G. (2010). Specific control of Pseudomonas aeruginosa surface-associated behaviors by two c-di-GMP diguanylate cyclases. Mbio *1*.

Morrison, S., and Kimble, J. (2006). Asymmetric and symmetric stem-cell divisions in development and cancer. Nature *441*, 1068-74.

Murray, T.S., Kazmierczak, B.I., Murray, T.S., and Kazmierczak, B.I. (2006). FlhF Is Required for Swimming and Swarming in Pseudomonas aeruginosa. Journal Of Bacteriology *188*, 1-11.

Navarro, M., Nabanita, Bae, N., Wang, Q., and Sondermann, H. (2009). Structural analysis of the GGDEF-EAL domain-containing c-di-GMP receptor FimX. Structure (London, England : 1993) *17*, 1104-16.

O'Brien, E., and Bennett, P. (1972). Structure of straight flagella from a mutant Salmonella. Journal Of Molecular Biology *70*, 133-52.

O'Connor, J.R., Kuwada, N.J., Huangyutitham, V., Wiggins, P.A., and Harwood, C.S. (2012). Surface sensing and lateral subcellular localization of WspA, the receptor in a chemosensory-like system leading to c-di-GMP production. Molecular Microbiology *86*, 1-10.

Oliveira, R., Terrin, A., Benedetto, G., Cannon, R., Koh, W., Kim, M., Zaccolo, M., and Blackwell, K. (2010). The role of type 4 phosphodiesterases in generating microdomains of cAMP: large scale stochastic simulations. PLOS ONE *5*, e11725.

Park, D. (2005). The microbiology of ventilator-associated pneumonia. Respiratory Care *50*, 742-63; discussion 763-5.

Paul, K., Nieto, V., Carlquist, W.C., Blair, D.F., and Harshey, R.M. (2010). The c-di-GMP Binding Protein YcgR Controls Flagellar Motor Direction and Speed to Affect Chemotaxis by a "Backstop Brake" Mechanism. Molecular Cell *38*, 1-12.

Paul, R., Weiser, S., Amiot, N.C., Chan, C., Schirmer, T., Giese, B., and Jenal, U. (2004). Cell cycle-dependent dynamic localization of a bacterial response regulator with a novel di-guanylate cyclase output domain. Genes &Amp; Development *18*, 1-14.

Pedro, M., Quintela, J., Höltje, J., and Schwarz, H. (1997). Murein segregation in Escherichia coli. Journal Of Bacteriology *179*, 2823-34.

Petrova, O.E., and Sauer, K. (2012a). PAS Domain Residues and Prosthetic Group Involved in BdlA-Dependent Dispersion Response by Pseudomonas aeruginosa Biofilms. Journal Of Bacteriology *194*, 5817-5828.

Petrova, O., and Sauer, K. (2012b). Dispersion by Pseudomonas aeruginosa requires an unusual posttranslational modification of BdlA. Proceedings Of The National Academy Of Sciences Of The United States Of America *109*, 16690-5.

Ping, L. (2010). The asymmetric flagellar distribution and motility of Escherichia coli. Journal Of Molecular Biology *397*, 906-16.

Pultz, I.S., Christen, M., Kulasekara, H.D., Kennard, A., Kulasekara, B., and Miller, S.I. (2012). The response threshold of Salmonella PilZ domain proteins is determined by their binding affinities for c-di-GMP. Molecular Microbiology *86*, 1-17.

Qi, Y., Chuah, M., Dong, X., Xie, K., Luo, Z., Tang, K., and Liang, Z. (2011). Binding of cyclic diguanylate in the non-catalytic EAL domain of FimX induces a long-range conformational change. The Journal Of Biological Chemistry *286*, 2910-7.

Qi, Y., Xu, L., Dong, X., Yau, Y., Ho, C., Koh, S., Shochat, S., Chou, S., Tang, K., and Liang, Z. (2012). Functional divergence of FimX in PilZ binding and type IV pilus regulation. Journal Of Bacteriology *194*, 5922-31.

Quon, K., Yang, B., Domian, I., Shapiro, L., and Marczynski, G. (1998). Negative control of bacterial DNA replication by a cell cycle regulatory protein that binds at the chromosome origin. Proceedings Of The National Academy Of Sciences Of The United States Of America *95*, 120-5.

Reinhardt, A., Köhler, T., Wood, P., Rohner, P., Dumas, J., Ricou, B., and Delden, C. (2007). Development and persistence of antimicrobial resistance in Pseudomonas aeruginosa: a longitudinal observation in mechanically ventilated patients. Antimicrobial Agents And Chemotherapy *51*, 1341-50.

Rietsch, A., Vallet-Gely, I., Dove, S., and Mekalanos, J. (2005). ExsE, a secreted regulator of type III secretion genes in Pseudomonas aeruginosa. Proceedings Of The National Academy Of Sciences Of The United States Of America *102*, 8006-11.

Ringgaard, S., Schirner, K., Davis, B., and Waldor, M. (2011). A family of ParA-like ATPases promotes cell pole maturation by facilitating polar localization of chemotaxis proteins. Genes &Amp; Development *25*, 1544-55.

Rochais, F., Abi-Gerges, A., Horner, K., Lefebvre, F., Cooper, D., Conti, M., Fischmeister, R., and Vandecasteele, G. (2006). A specific pattern of phosphodiesterases controls the cAMP signals generated by different Gs-coupled receptors in adult rat ventricular myocytes. Circulation Research *98*, 1081-8.

Ross, P., Weinhouse, H., Aloni, Y., Michaeli, D., Weinberger-Ohana, P., Mayer, R., Braun, S., Vroom, E., Marel, G., Boom, J., et al. (1987). Regulation of cellulose synthesis in Acetobacter xylinum by cyclic diguanylic acid. Nature *325*, 279-81.

Rotem, E., Loinger, A., Ronin, I., Levin-Reisman, I., Gabay, C., Shoresh, N., Biham, O., and Balaban, N. (2010). Regulation of phenotypic variability by a threshold-based mechanism underlies bacterial persistence. Proceedings Of The National Academy Of Sciences Of The United States Of America *107*, 12541-6.

Roy, A.B., Petrova, O.E., and Sauer, K. (2012). The Phosphodiesterase DipA (PA5017) Is Essential for Pseudomonas aeruginosa Biofilm Dispersion. Journal Of Bacteriology *194*, 2904-2915.

Rudel, D., and Sommer, R. (2003). The evolution of developmental mechanisms. Developmental Biology *264*, 15-37.

Ryder, C., Byrd, M., and Wozniak, D. (2007). Role of polysaccharides in Pseudomonas aeruginosa biofilm development. Current Opinion In Microbiology *10*, 644-8.

Ryjenkov, D., Simm, R., Römling, U., and Gomelsky, M. (2006). The PilZ domain is a receptor for the second messenger c-di-GMP: the PilZ domain protein YcgR controls motility in enterobacteria. The Journal Of Biological Chemistry *281*, 30310-4.

Römling, U., Galperin, M., and Gomelsky, M. (2013). Cyclic di-GMP: the First 25 Years of a Universal Bacterial Second Messenger. Microbiology And Molecular Biology Reviews : MMBR *77*, 1-52.

Schmidt, J., Müsken, M., Becker, T., Magnowska, Z., Bertinetti, D., Möller, S., Zimmermann, B., Herberg, F.W., Jänsch, L., and Häussler, S. (2011). The Pseudomonas aeruginosa chemotaxis methyltransferase CheR1 impacts on bacterial surface sampling. PLOS ONE *6*, 1-11.

Schniederberend, M., Abdurachim, K., Murray, T., and Kazmierczak, B. (2013). The GTPase activity of FlhF is dispensable for flagellar localization, but not motility, in Pseudomonas aeruginosa. Journal Of Bacteriology *195*, 1051-60.

Seshasayee, A., Fraser, G., and Luscombe, N. (2010). Comparative genomics of cyclic-di-GMP signalling in bacteria: post-translational regulation and catalytic activity. Nucleic Acids Research *38*, 5970-81.

Shikuma, N., Fong, J., and Yildiz, F. (2012). Cellular levels and binding of c-di-GMP control subcellular localization and activity of the Vibrio cholerae transcriptional regulator VpsT. Plos Pathogens *8*, e1002719.

Simm, R., Morr, M., Kader, A., Nimtz, M., and Römling, U. (2004). GGDEF and EAL domains inversely regulate cyclic di-GMP levels and transition from sessility to motility. Molecular Microbiology *53*, 1123-34.

Skerker, J., and Berg, H. (2001). Direct observation of extension and retraction of type IV pili. Proceedings Of The National Academy Of Sciences Of The United States Of America *98*, 6901-4.

Smith, E., Buckley, D., Wu, Z., Saenphimmachak, C., Hoffman, L., D'Argenio, D., Miller, S., Ramsey, B., Speert, D., Moskowitz, S., et al. (2006). Genetic adaptation by Pseudomonas aeruginosa to the airways of cystic fibrosis patients. Proceedings Of The National Academy Of Sciences Of The United States Of America *103*, 8487-92.

Smith, K., Lipchock, S., Ames, T., Wang, J., Breaker, R., and Strobel, S. (2009). Structural basis of ligand binding by a c-di-GMP riboswitch. Nature Structural &Amp; Molecular Biology *16*, 1218-23.

Solano, C., García, B., Latasa, C., Toledo-Arana, A., Zorraquino, V., Valle, J., Casals, J., Pedroso, E., and Lasa, I. (2009). Genetic reductionist approach for dissecting individual roles of GGDEF proteins within the c-di-GMP signaling network in Salmonella. Proceedings Of The National Academy Of Sciences Of The United States Of America *106*, 7997-8002.

Solano, C., García, B., Valle, J., Berasain, C., Ghigo, J., Gamazo, C., and Lasa, I. (2002). Genetic analysis of Salmonella enteritidis biofilm formation: critical role of cellulose. Molecular Microbiology *43*, 793-808.

Sondermann, H., Shikuma, N., and Yildiz, F. (2012). You've come a long way: c-di-GMP signaling. Current Opinion In Microbiology *15*, 140-6.

Sourjik, V., and Wingreen, N. (2012). Responding to chemical gradients: bacterial chemotaxis. Current Opinion In Cell Biology *24*, 262-8.

Sowa, Y., and Berry, R. (2008). Bacterial flagellar motor. Quarterly Reviews Of Biophysics *41*, 103-32.

Starkey, M., Hickman, J., Ma, L., Zhang, N., Long, S., Hinz, A., Palacios, S., Manoil, C., Kirisits, M., Starner, T., et al. (2009). Pseudomonas aeruginosa rugose small-colony variants have adaptations that likely promote persistence in the cystic fibrosis lung. Journal Of Bacteriology *191*, 3492-503.

Suzuki, T., and Iino, T. (1980). Isolation and characterization of multiflagellate mutants of Pseudomonas aeruginosa. Journal Of Bacteriology *143*, 1-10.

Tarutina, M., Ryjenkov, D., and Gomelsky, M. (2006). An unorthodox bacteriophytochrome from Rhodobacter sphaeroides involved in turnover of the second messenger c-di-GMP. The Journal Of Biological Chemistry *281*, 34751-8.

Taskén, K., and Aandahl, E. (2004). Localized effects of cAMP mediated by distinct routes of protein kinase A. Physiological Reviews *84*, 137-67.

Terrin, A., Benedetto, G., Pertegato, V., Cheung, Y., Baillie, G., Lynch, M., Elvassore, N., Prinz, A., Herberg, F., Houslay, M., et al. (2006). PGE(1) stimulation of HEK293 cells generates multiple contiguous domains with different [cAMP]: role of compartmentalized phosphodiesterases. The Journal Of Cell Biology *175*, 441-51.

Thevenaz, P., Ruttimann, U.E., and Unser, M. A pyramid approach to subpixel registration based on intensity. IEEE Transactions On Image Processing *7*, 1-15.

Tischler, A., and Camilli, A. (2004). Cyclic diguanylate (c-di-GMP) regulates Vibrio cholerae biofilm formation. Molecular Microbiology *53*, 857-69.

Toutain, C., Zegans, M., and O'Toole, G. (2005). Evidence for two flagellar stators and their role in the motility of Pseudomonas aeruginosa. Journal Of Bacteriology *187*, 771-7.

Trimble, M., and McCarter, L. (2011). Bis-(3“-5”)-cyclic dimeric GMP-linked quorum sensing controls swarming in Vibrio parahaemolyticus. Proceedings Of The National Academy Of Sciences Of The United States Of America *108*, 18079-84.

Tsokos, C., and Laub, M. (2012). Polarity and cell fate asymmetry in Caulobacter crescentus. Current Opinion In Microbiology *15*, 744-50.

Turner, L., Ryu, W., and Berg, H. (2000). Real-time imaging of fluorescent flagellar filaments. Journal Of Bacteriology *182*, 2793-801.

Turner, L., Zhang, R., Darnton, N.C., and Berg, H.C. (2010). Visualization of Flagella during bacterial Swarming. Journal Of Bacteriology *192*, 3259-67.

Viollier, P., Sternheim, N., and Shapiro, L. (2002). A dynamically localized histidine kinase controls the asymmetric distribution of polar pili proteins. The EMBO Journal *21*, 4420-8.

Wassmann, P., Chan, C., Paul, R., Beck, A., Heerklotz, H., Jenal, U., and Schirmer, T. (2007). Structure of BeF3- -modified response regulator PleD: implications for diguanylate cyclase activation, catalysis, and feedback inhibition. Structure (London, England : 1993) *15*, 915-27.

Weber, H., Pesavento, C., Possling, A., Tischendorf, G., and Hengge, R. (2006). Cyclic-di-GMP-mediated signalling within the sigma network of Escherichia coli. Molecular Microbiology *62*, 1014-34.

Wheeler, R., and Shapiro, L. (1999). Differential localization of two histidine kinases controlling bacterial cell differentiation. Molecular Cell *4*, 683-94.

Whitney, J., Colvin, K., Marmont, L., Robinson, H., Parsek, M., and Howell, P. (2012). Structure of the cytoplasmic region of PelD, a degenerate diguanylate cyclase receptor that regulates

exopolysaccharide production in Pseudomonas aeruginosa. The Journal Of Biological Chemistry *287*, 23582-93.

Woude, M. (2011). Phase variation: how to create and coordinate population diversity. Current Opinion In Microbiology *14*, 205-11.

Xia, Z., and Liu, Y. (2001). Reliable and Global Measurement of Fluorescence Resonance Energy Transfer Using Fluorescence Microscopes. Biophysical Journal *81*, 1-8.

Xie, L., Altindal, T., Chattopadhyay, S., and Wu, X. (2011). From the Cover: Bacterial flagellum as a propeller and as a rudder for efficient chemotaxis. Proceedings Of The National Academy Of Sciences Of The United States Of America *108*, 2246-51.

Zaccolo, M., and Pozzan, T. (2002). Discrete microdomains with high concentration of cAMP in stimulated rat neonatal cardiac myocytes. Science (New York, N.Y.) *295*, 1711-5.

Nabanita, Pirruccello, M., Krasteva, P., Bae, N., Raghavan, R., and Sondermann, H. (2008). Phosphorylation-independent regulation of the diguanylate cyclase WspR. Plos Biology *6*, e67.